

The human visual cortex response to melanopsin-directed stimulation is accompanied by a distinct perceptual experience

Manuel Spitschan¹, Andrew S. Bock², Jack Ryan², Giulia Frazzetta², David H. Brainard¹ and Geoffrey K. Aguirre^{2,*}

¹Department of Psychology, University of Pennsylvania, Philadelphia, PA 19104, USA

²Department of Neurology, Perelman School of Medicine, University of Pennsylvania, Philadelphia, PA 19104, USA

*Corresponding author: aguirreg@mail.med.upenn.edu

Number of Pages: 20

Number of Figures: 5

Number of Tables: 0

Number of words for Abstract: 147

Number of words for Main text: 4150

Competing financial interests: G.K.A., D.H.B., and M.S. are listed as inventors on a patent application filed by the Trustees of the University of Pennsylvania on September 11, 2015 (U.S. Patent Application No. 14/852,001, "Robust Targeting Of Photosensitive Molecules"). The authors declare no other competing financial interests.

Acknowledgements: This work was supported by the National Institutes of Health (Grant R01 EY024681 to G.K.A. and D.H.B., Core Grant for Vision Research P30 EY001583, and Neuroscience Neuroimaging Center Core Grant P30 NS045839), the Department of Defense (Grant MR141251 to G.K.A). We thank Fred Letterio for technical assistance, and Andrew S. Olsen for his assistance with data collection.

Contributions: M.S., D.H.B., and G.K.A. conceived the project. M.S. and G.K.A. designed the fMRI experiments. J.R., D.H.B., and G.K.A. designed the perceptual experiment. M.S. and D.H.B. designed the spectral modulations. M.S., A.S.B., J.R., G.F. and G.K.A. collected fMRI data. G.F. collected pupillometry data. J.R. collected perceptual data. M.S., A.S.B. and G.F. analyzed fMRI data. M.S. and G.F. analyzed pupillometry data. G.K.A. implemented temporal models for the fMRI and pupillometry data. D.H.B., J.R. and G.K.A. analyzed perceptual data. M.S. analyzed the effects of biological variability upon photoreceptor contrast. G.K.A. created the figures. M.S. and G.K.A. wrote the manuscript with contributions from J.R., A.S.B., G.F. and D.H.B.

37 **Abstract**

38 The photopigment melanopsin supports reflexive visual functions in people, such as pupil con-
39 striction and circadian photoentrainment. What contribution melanopsin makes to conscious
40 visual perception is less studied. We devised a stimulus that targeted melanopsin separately
41 from the cones using pulsed (3 s) spectral modulations around a photopic background. Pupil-
42 lometry confirmed that the melanopsin stimulus drives a retinal mechanism distinct from lu-
43 minance. In each of four subjects, a functional MRI response in area V1 was found. This
44 response scaled with melanopic contrast and was not easily explained by imprecision in the
45 silencing of the cones. Twenty additional subjects then observed melanopsin pulses and pro-
46 vided a structured rating of the perceptual experience. Melanopsin stimulation was described
47 as an unpleasant, blurry, minimal brightening that quickly faded. We conclude that isolated
48 stimulation of melanopsin is likely associated with a response within the cortical visual path-
49 way and with an evoked conscious percept.

50 Introduction

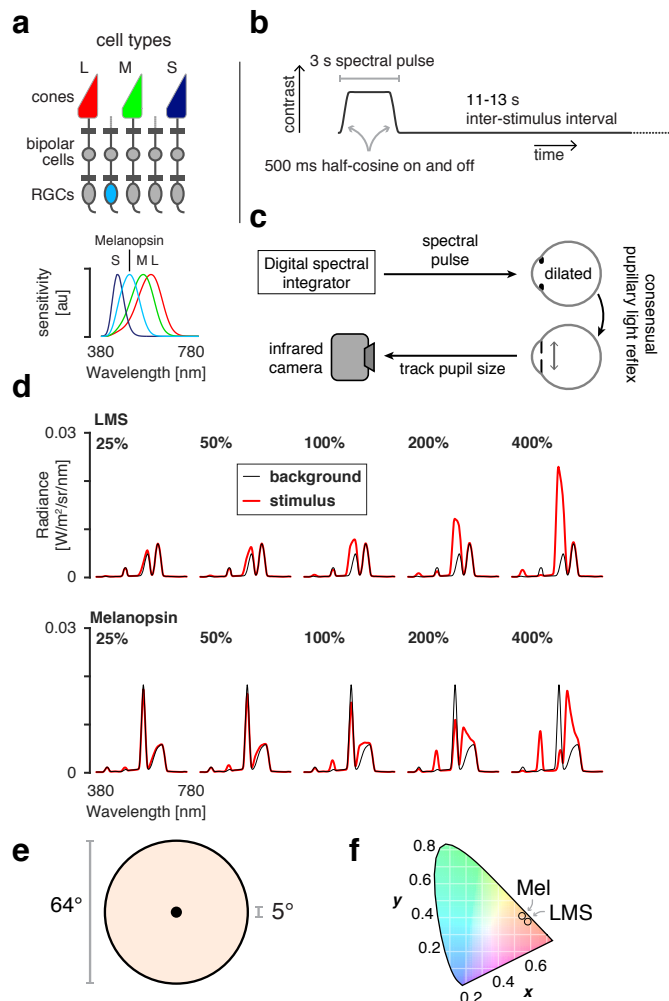
51 Human visual perception under daylight conditions is well described by the combination of sig-
52 nals from the short (S)-, medium (M)-, and long (L)-wavelength cones.¹ Melanopsin-containing,
53 intrinsically photosensitive retinal ganglion cells (ipRGCs) are also active in bright light (Figure
54 1a). The ipRGCs have notably prolonged responses to changes in light level, and thus signal
55 retinal irradiance in their tonic firing.² Studies in rodents, non-human primates, and people
56 have emphasized the role of the ipRGCs in reflexive, non-image forming visual functions that
57 integrate information over tens of seconds to hours, such as circadian photoentrainment, pupil
58 control, and somatosensory discomfort from bright light.^{3–6}

59 Relatively unexamined is the effect of melanopsin phototransduction upon visual percep-
60 tion, which operates at shorter timescales. In addition to tonic firing, ipRGCs exhibit transient
61 responses to flashes of light with an onset latency as short as 200 ms.⁷ Several ipRGC sub-
62 types project to the lateral geniculate nucleus, where they are found to drive both transient and
63 tonic neural responses.⁸ As the geniculate is the starting point of the cortical pathway for visual
64 perception, it is possible that ipRGC activity has an explicitly visual perceptual correlate.

65 Here we examine whether isolated melanopsin stimulation drives responses within human
66 visual cortex, and characterize the associated perceptual experience. Our approach uses
67 balanced modulations of the spectral content of a light stimulus, allowing melanopsin to be tar-
68 geted separately from the cones in visually normal subjects.^{9,10} We also studied the converse
69 stimulus, which drives the cone-based luminance channel while minimizing melanopsin stim-
70 ulation. We collected blood oxygen level dependent (BOLD) functional magnetic resonance
71 imaging (fMRI) while subjects viewed brief (three-second) pulses of these spectral modula-
72 tions. Concurrent infrared pupillometry was used to confirm that our stimuli elicit responses
73 from distinct retinal mechanisms. Finally, we characterized the perceptual experience of se-
74 lective melanopsin-directed stimulation, and examined whether this experience is distinct from
75 that caused by stimulation of the cones.

Figure 1: Overview and experimental design

(a) *Top* The L, M, and S cones, and melanopsin-containing ipRGCs, mediate vision at daytime light levels. *Bottom* The spectral sensitivities of these photoreceptor classes. **(b)** Multiple 3-second, pulsed spectral modulations were presented, windowed by a 500 ms half-cosine at onset and offset, and followed by an 11-13 s ISI. A given experiment presented either a single contrast level, or multiple contrast levels in a counter-balanced order. **(c)** During fMRI scanning, subjects viewed pulsed spectral modulations, produced by a digital spectral integrator, with their pharmacologically dilated right eye. The consensual pupil response of the left eye was recorded in some experiments. **(d)** Stimulus spectra. Changes between a background spectrum (black) and modulation spectra (red) targeted a given photoreceptor channel with varying degrees of contrast. *Top* Spectra targeting the L, M, and S cones and thus the post-receptoral luminance channel. We use the terms “LMS” and “luminance” interchangeably to describe this stimulus. The nominal melanopic contrast for these modulations was zero. *Bottom* The corresponding spectra for stimuli targeting melanopsin. The nominal L-, M-, and S-cone contrast of these stimuli was zero. **(e)** Spectra were presented on a uniform field of 64° (visual angle) diameter. Subjects fixated the center of a 5° masked region, minimizing stimulation of the macula. **(f)** The calculated chromaticity of the background spectra was approximately matched for the LMS and melanopsin directed stimuli, and had a light-orange hue.



76 Results

77 Four subjects were studied in multiple experiments while they viewed intermittent pulses of
 78 spectral contrast directed at either the post-receptoral luminance pathway (LMS, equal con-
 79 trast on cones) or the melanopsin containing ipRGCs (Figure 1a, 1b). During functional MRI
 80 scanning, subjects viewed these stimuli with their pharmacologically dilated right eye; in some
 81 experiments the consensual response of the left pupil was also recorded with an infra-red cam-
 82 era (Figure 1c). Different stimuli produced contrast upon the targeted photoreceptors between
 83 25% and 400% (Figure 1d; additional stimulus details in Figure S1). The subject maintained
 84 fixation upon a masked central disk (Figure 1e), while spectral changes occurred in the visual
 85 periphery against a background that was depleted in short-wavelength light and thus had a
 86 light-orange hue (Figure 1f).

87 **V1 cortex responds to melanopsin contrast**

88 We first examined the extent of cortical response to high-contrast spectral pulses. Each sub-
89 ject viewed approximately 200 pulses each of the 400% luminance and melanopsin stimuli.
90 We measured the reliability of the evoked response within subject, and then at a second level
91 across subjects and the two hemispheres. Pulses of luminance contrast that minimized melano-
92 psin stimulation (Figure 2a) produced responses in the early cortical visual areas, gener-
93 ally corresponding to the retinotopic projection of the stimulated portion of the visual field.¹¹
94 Spectral pulses directed at melanopsin that minimized cone stimulation also evoked responses
95 within the visual cortex (Figure 2b). In subsequent experiments, we examined the evoked re-
96 sponses to luminance and melanopsin stimulation within a region of interest in V1 cortex that
97 lies entirely within the retinotopic projection of the stimulated visual field. The time-series data
98 and evoked responses from within this region for the initial, 400% contrast only experiment can
99 be found in Figure S2.

100 The ipRGCs modulate their activity in relation to retinal irradiance.² If the visual cortex en-
101 codes information from the ipRGCs, we would expect that the degree of BOLD fMRI response
102 should reflect variation in the degree of melanopsin stimulation, similar to the modulation of
103 cortical response seen to variation in luminance contrast.¹² Each of the four observers was
104 studied again, this time with spectral pulses that varied in the degree of contrast upon the LMS
105 or melanopsin channels. Figure 1c shows an example of the data obtained from the V1 region
106 of interest in response to luminance pulses during one scan run for one observer. The time-
107 series was fit with a Fourier basis set that estimated the shape of the BOLD fMRI response
108 evoked by stimuli of each contrast level. Figure 1d presents the time-series data and evoked
109 responses for the four subjects during luminance stimulation. Luminance pulses evoked con-
110 sistent responses in the V1 region of interest, with a steadily increasing amplitude of evoked
111 response across contrast levels. Variation in melanopic contrast (Figure 1e) produced similar
112 data, with an increasing amplitude of BOLD fMRI response to larger contrasts.

113 We fit the evoked responses at each contrast level for each subject using an empirical mea-
114 sure of the subject's hemodynamic response function, along with parameters that controlled
115 the duration of an underlying neural response and the amplitude of the evoked BOLD fMRI
116 signal (Figure S3). We obtained the amplitude of response as a function of contrast for each
117 subject and each stimulus (Figure 3; LMS and melanopsin; grey and blue lines, respectively).

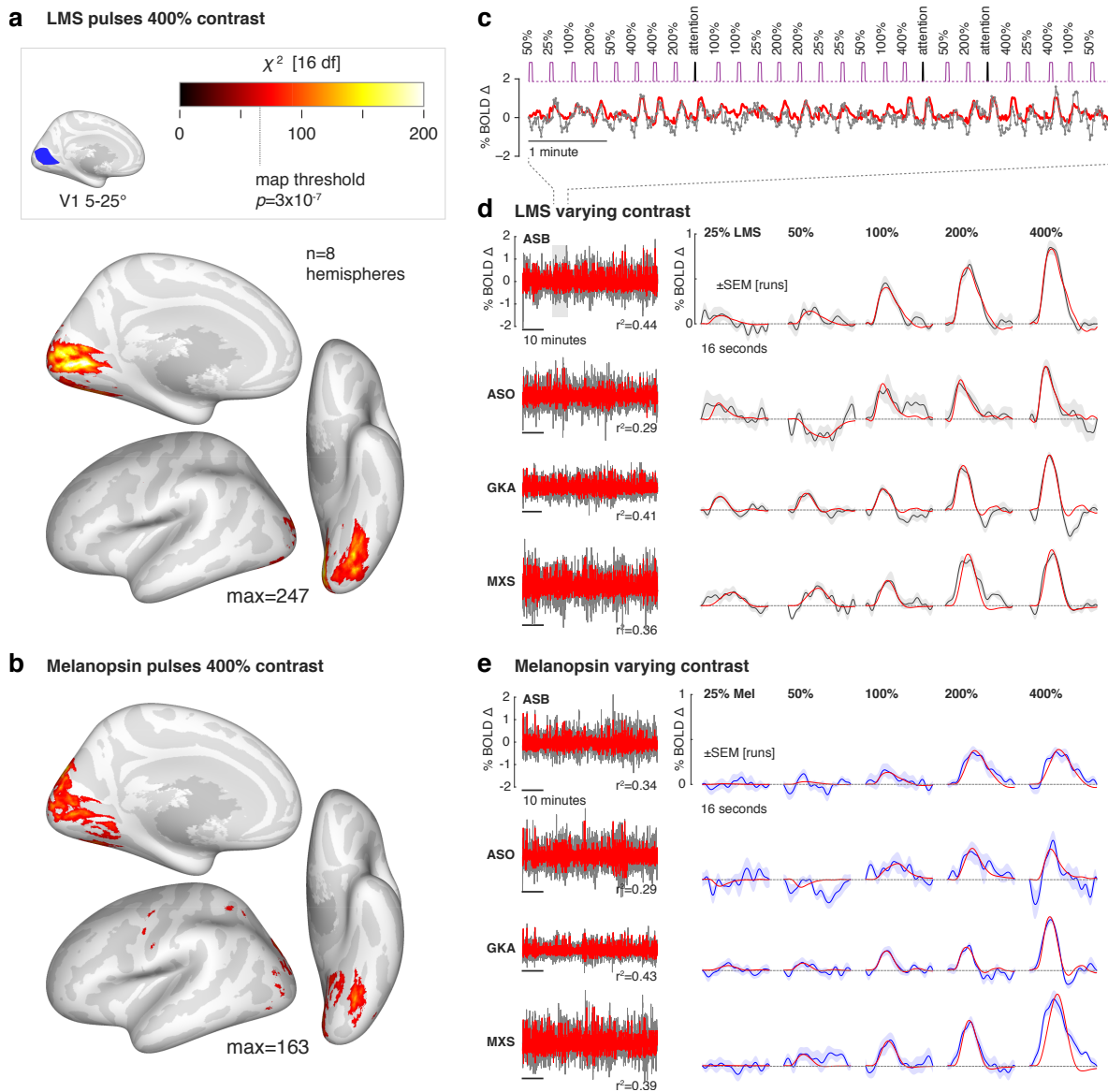
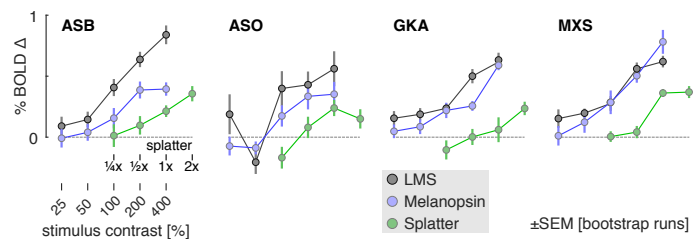


Figure 2: Visual cortex responses to LMS and melanopsin contrast. (a) Cortical response to pulses of 400% LMS contrast across subjects and hemispheres. Threshold corresponds to a map-wise $\alpha = 0.05$ (Bonferroni corrected for the number of vertices). Inset *top* is the region of V1 cortex with retinotopic representation corresponding to the visual field range of 5-25° radial eccentricity, indicated in blue. Subsequent analyses examine the mean signal from this region. (b) The corresponding surface map obtained in response to 400% Melanopsin contrast pulses. (c) Example fit (red) of the Fourier basis set to a portion of the BOLD fMRI time-series data (gray). (d) Responses to LMS stimulation of varying contrast. *Left* The BOLD fMRI time-series data from the area V1 region for each subject (black), following pre-processing to remove nuisance effects. A Fourier basis set modeled (red) the mean evoked response to each contrast level with the r^2 value of the model fit indicated. *Right* The evoked responses for each subject and stimulus level (black), and SEM of the response across the 9-11 scanning runs performed in each subject (shaded region). The responses were fit by a model (red) that convolved a step function of neural activity by the hemodynamic response function measured for each subject (Figure S3). (e) The corresponding responses within the V1 region to melanopsin stimulation of varying contrast.

Figure 3: V1 BOLD fMRI response by stimulus contrast. The amplitude of evoked response with the V1 region was obtained for each subject and contrast level for the luminance (gray), melanopsin (cyan), and “splatter” (green) stimulus conditions. The 1x splatter condition presented cone contrast equal to the maximal inadvertent contrast (resulting from imperfections in device control) measured in validated spectra in the melanopsin experiments.



118 As suggested by the evoked responses in Figure 2, the measured amplitude increased as a
119 function of contrast for both luminance and melanopsin stimulation for all four observers. While
120 we modeled the duration of underlying neural activity, the results did not support the claim of a
121 distinct temporal response to melanopsin stimulation (Figure S4).

122 While the melanopsin-directed spectral pulses were designed to produce no differential
123 stimulation of the cones, biological variation and inevitable imperfection in device control results
124 in some degree of unwanted cone stimulation (termed “splatter”).^{9,10,13} We considered the
125 possibility that what appeared to be a visual cortex response to melanopsin contrast was in
126 fact a response to the small amount of cone contrast inadvertently produced by our nominally
127 cone silent spectral pulses.

128 We obtained spectroradiometric measurements of the stimuli that were actually produced
129 by our device at the time of the BOLD fMRI experiment for each subject. For each of these
130 measurements we calculated the inadvertent contrast that the cones would have experienced
131 within these 400% melanopsin modulations in a biologically typical subject. We took the max-
132 imum contrast values calculated for the measurements across subjects, and created a new
133 spectral pulse that was designed to have no melanopsin stimulation, but to have cone con-
134 trast equal to this estimate of inadvertent contrast. Scaled versions of this modulation corre-
135 sponded to logarithmically-spaced larger (2x) and smaller ($\frac{1}{2}$ x, $\frac{1}{4}$ x) multiples of the “splatter”
136 contrast. We again studied the four subjects with BOLD fMRI while they viewed these stimuli,
137 and measured the amplitude of response as a function of splatter contrast (Figure 3, green
138 line). In all four subjects, the melanopsin response function was larger than the splatter re-
139 sponse function. This indicates that the cortical response to melanopsin cannot be explained
140 entirely by imperfection in stimulus generation. We then explored if biological variability could
141 result in a greater degree of inadvertent cone contrast than our analysis of device imprecision
142 alone would suggest. Our characterization of the stimuli in terms of cone contrast relies upon
143 assumed values for several biological variables, including lens density, peak spectral sensitivity

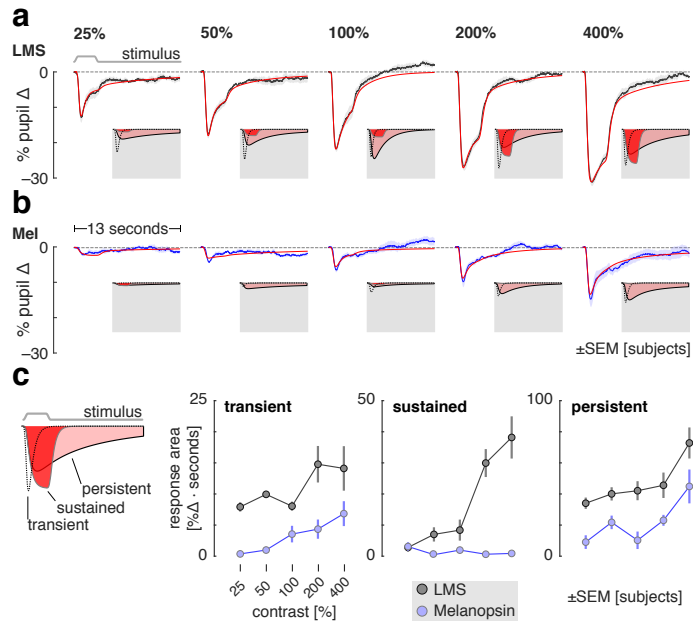
144 of the cone photopigments, their density, and the density of macular pigment. We conducted
145 simulations in which we calculated the degree of inadvertent cone contrast that would have
146 resulted given deviations from our assumptions, following estimated distributions of these bio-
147 logical variables.¹⁴ We find that it is very unlikely (approximately one chance in 100,000) that
148 the responses observed in the four subjects could have resulted solely from inadvertent cone
149 contrast (Figure S5).

150 The spectral sensitivity of the rod photoreceptors overlaps extensively with that of mela-
151 nopsin. The background used for our melanopsin-directed stimuli was $3.5 \log_{10}$ scotopic
152 Trolands (scot Td), nominally at or above the rod saturation threshold, found to be $3.0 \log_{10}$
153 scot Td (Figure 2 of Adelson 1982)¹⁵ or $3.3\text{-}3.7 \log_{10}$ scot Td (Aguilar & Styles 1954).¹⁶ There-
154 fore, we expect in our experiments that there is no, or minimal, time-varying signal contributed
155 by the rods. We attempted in a control experiment to further exclude this possibility by mak-
156 ing use of an assumed difference in temporal sensitivity of the rods and melanopsin, but this
157 experiment was uninformative (Figure S6). We return to this topic in the discussion.

158 A prior functional MRI study that presented a 50% Weber contrast melanopsin modula-
159 tion did not find responses within the visual cortex, but did observe BOLD fMRI responses
160 within the frontal eye fields.¹⁷ The authors speculated that melanopsin stimulation produces
161 changes in alertness that manifest as these cortical responses, although eye movements were
162 not recorded during their study. In our whole brain analysis (Figure 2a, 2b) we find responses
163 within the frontal eye fields for both the luminance and melanopsin pulses at lowered map
164 thresholds (unthresholded maps available from <http://neurovault.org/collections/2459/>). We
165 considered the possibility that our stimulus pulses might cause subjects to briefly increase
166 or decrease saccadic eye movements. We measured variation in eye position during the 3 s
167 of stimulation and during the interstimulus interval (Figure S7). Subjects consistently reduced
168 eye movements during the luminance and melanopsin stimulation periods as compared to the
169 inter-stimulus-interval. This effect may account for the frontal eye field responses in our data
170 and in the prior report.¹⁷ As eye movements alone can evoke responses in visual cortex,¹⁸ we
171 considered that a systematic difference in eye movements across contrast levels might con-
172 found our finding of a contrast response in area V1. However, no eye movement difference
173 was seen as a function of contrast level or stimulus type (LMS vs. melanopsin).

Figure 4: Consensual pupil responses to LMS and melanopsin stimulation.

The consensual pupil response of the left eye was measured during stimulation of the pharmacologically dilated right eye. **(a)** The mean (across subjects) pupil response evoked by LMS stimulation of varying contrast levels (black), with SEM across subjects (shaded). The evoked response was fit with a three component, six-parameter model (red). The three components that model each response are shown inset on a gray field. **(b)** The corresponding mean pupil responses evoked by melanopsin stimulation of varying contrast levels. **(c)** Amplitude of the three model components as a function of stimulus contrast. Inset *left* is an illustration of the three model components. *Right* gain parameter for each model component as a function of contrast for LMS (gray) and melanopsin (blue) stimulation.



174 **Different kinetics of pupil response to melanopic and luminance pulses**

175 We have previously shown using sinusoidal spectral modulations that pupil responses to mela-
176 nopsin stimulation have different temporal properties as compared to the responses evoked
177 by modulations of luminance.¹⁰ In the current study, we recorded pupil responses to pulsed
178 spectral modulations during the presentation of melanopsin and LMS stimulation of varying
179 contrast. We examined these pupil responses for qualitative differences in the time course of
180 the response. Such a demonstration would increase confidence that our stimuli target distinct
181 retinal mechanisms.

182 The average pupil response was obtained for each contrast level and stimulus type. In the
183 across-subject averages (Figure 4a; individual subject data in Figure S8), an evoked response
184 to LMS stimulation is seen at even the lowest contrast level (25%). As LMS contrast grows,
185 the evoked pupil response becomes larger, with distinct features corresponding to the onset
186 and the offset of the 3 s stimulus pulse. The response to melanopsin contrast (Figure 4b)
187 begins smaller, but also increases with contrast. Unlike the pupil response to LMS contrast, it
188 is difficult to discern an indication of stimulus offset in the extended response to melanopsin
189 stimulation.

190 We quantified these observations by fitting a temporal model (Figure S9) to the average
191 evoked pupil responses. The model has three temporally distinct components that capture an
192 initial transient constriction of the pupil at stimulus onset, a sustained response that tracks the
193 stimulus profile, and a persistent response as the pupil slowly re-dilates in the seconds after

194 stimulus offset (shown inset in each plot panel in Figure 4a and 4b, and schematically inset
195 left in Figure 4c). The amplitude of each of these components was measured as a function of
196 contrast for the LMS and melanopsin stimuli (Figure 4c; temporal parameter values in Figure
197 S10). The amplitude of both the initial transient and persistent response increase with LMS
198 and melanopsin contrast. The behavior of the sustained component, however, is different for
199 the two types of stimulation. Luminance contrast produces steadily increasing sustained pupil
200 constriction that is time-locked to the profile of the stimulus. In contrast, there is essentially no
201 component of this kind in the melanopsin-driven pupil response. This behavior is in keeping
202 with the temporally low-pass properties of the melanopsin system.¹⁰

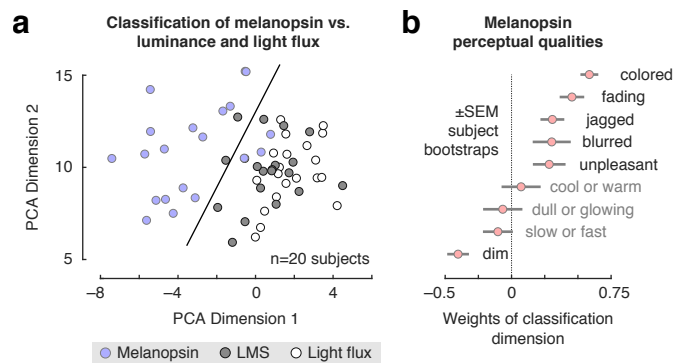
203 **Melanopsin stimulation evokes a distinct visual percept**

204 We find that a melanopsin-directed spectral pulse evokes a measurable response in the visual
205 cortex. This suggests that people have conscious perceptual awareness of stimulation of the
206 ipRGCs. Prior studies have found that melanopsin contrast contributes to a sensation of bright-
207 ness, as subjects rate lights that contain melanopsin and luminance contrast as brighter than
208 a light with luminance contrast alone.¹⁹ We were curious as to whether the perception of se-
209 lective melanopsin-directed contrast appears simply as the typical experience of “brightness”
210 conveyed by the luminance channel, or if there is a distinct perceptual experience associated
211 with our melanopsin-directed stimulus.

212 We recruited 20 subjects naïve to the hypotheses of the study and asked them to view
213 400% contrast pulses of LMS, melanopsin, and a stimulus changing in power equally across all
214 wavelengths, thus stimulating both melanopsin and luminance channels (“light flux”). Subjects
215 were asked to rate nine perceptual qualities of the light pulse, each quality defined by a pair
216 of antonyms (e.g., dim to bright). Subjects were not informed of the different identities of the
217 stimuli, and the order was randomized as described in Online Methods. Subjects were also
218 invited to offer their free-form observations at the end of the study during a debriefing session
219 (summarized in Table S2).

220 A challenge of such measurements is the psychophysical sensitivity of the human visual
221 system to even small amounts of differential cone contrast.^{20,21} We implemented additional
222 stimulus calibration measures to further reduce spectral variation due to device instability (see
223 Online Methods). In the measured stimulus spectra, the amount of inadvertent cone contrast
224 in the melanopsin-directed stimulus due to imprecision in stimulus control was small (Figure

Figure 5: Perceptual ratings of melanopsin, luminance, and light flux. Subjects rated nine qualities of spectral pulses that targeted melanopsin, luminance, and their combination (light flux). **(a)** The set of perceptual ratings were subjected to a principal components analysis. Each point corresponds to the ratings provided by one subject for one stimulus type within the space defined by the first two dimensions of the PCA solution. A linear support-vector machine was trained to distinguish ratings for melanopsin stimulation from the other two stimulus types within this two-dimensional space. The classification boundary is shown. **(b)** The classification dimension (normal to the classification boundary) describes how melanopsin stimulation was perceived differently from light flux and luminance. The mean weights (across boot-strap resamples) that define the classification dimension are shown.



225 S11).

226 Subjects rated each property of each stimulus twice, allowing us to confirm that within-
227 subject reliability was high (across-subject mean Spearman correlation of test-retest reliability
228 = 0.73 ± 0.18 SD). Additionally, there was good subject agreement in the ratings (across-
229 subject mean Spearman correlation of ratings from one left-out subject to mean ratings of all
230 other subjects = 0.53 ± 0.13 SD).

231 Subjects consistently rated the melanopsin stimulus as perceptually distinct from the LMS
232 or light flux pulses (Table S1). We summarized these measurements by submitting them to a
233 principal components analysis (Figure 5a). The first and second dimensions explained 35%
234 and 19% of the variance in ratings, respectively. Within this space a support vector machine
235 could classify subject responses to melanopsin as distinct from those for LMS or light flux with
236 92% cross-validated accuracy. A plot of the weights that define the classification dimension
237 (Figure 5b) reveals the primary qualities of isolated melanopsin stimulation. To our naïve sub-
238 jects, and in our own experience, the onset of the melanopsin contrast appears as a somewhat
239 unpleasant, blurry, minimal brightening of the field. Most notably, however, this percept is fleet-
240 ing, and rapidly followed by a fading or loss of perception from the stimulus field. Many of the
241 subjects described the melanopsin stimulus pulse as being colored. This was typically with a
242 yellow-orange appearance, although three subjects reported a greenish percept.

243 The perceptual ratings of the LMS and light flux stimuli were quite similar, with the LMS
244 rated as having more color (again perhaps due to the inadvertent chromatic contrast present
245 in the stimulus; Figure S11) and the light flux as being somewhat brighter. Prior studies have

246 found that melanopsin contrast is additive to LMS contrast in the perception of brightness.¹⁹
247 In our data, this would be consistent with higher ratings on the dim-to-bright scale for light flux
248 pulses as compared to LMS. A post-hoc test supported this interpretation (Wilcoxon signed-
249 rank test of dim-to-bright ratings in Light Flux compared to LMS: $p=0.0088$).

250 **Discussion**

251 Our studies indicate a role for the melanopsin-containing ipRGCs in conscious human vision.
252 We find that high-contrast spectral exchanges designed to isolate melanopsin evoke responses
253 in human visual cortex. Pupil responses to these stimuli are distinct from those produced by
254 luminance contrast, consistent with separation of retinal mechanisms. The cortical response
255 is not easily explained by inadvertent stimulation of the cones and is associated with a distinct
256 perceptual experience.

257 Previous studies in rodents and humans with outer photoreceptor defects have suggested
258 that the visual cortex responds to melanopsin stimulation. Zaidi and colleagues reported the
259 case of an 87 year-old woman with autosomal-dominant cone-rod dystrophy who was able
260 to correctly report the presence of an intense, 480 nm 10 s light pulse, but not other wave-
261 lengths.²² Similarly, in mice lacking rods and cones, the presentation of a narrowband 447 nm
262 light evoked a hemodynamic (optical imaging) signal change in the rodent visual cortex, with a
263 slightly (1 s) delayed onset and a reduced amplitude as compared to the same measurement
264 in a wild-type mouse.²³ In our work we measured cortical and perceptual responses to isolated
265 melanopsin stimulation in the intact human visual system.

266 **A cortical response**

267 The melanopsin containing ipRGCs have broad projections to sub-cortical sites.²⁴ Studies in
268 the rodent and primate demonstrate as well projections to the lateral geniculate nucleus, where
269 evoked responses to melanopsin stimulation can be found.^{8,23,25} Whether these signals are
270 further transmitted to the visual cortex in normally sighted humans or non-human animals has
271 been unknown. We find that pulsed melanopsin stimulation evokes contrast-graded responses
272 within primary visual cortex. Responses to the highest (400%) contrast stimulus extend into ad-
273 jacent, retinotopically organized visual areas, including ventrally in the vicinity of the peripheral
274 representation for hV4 and VO1;²⁶ a similar distribution of cortical responses was observed to
275 luminance stimulation.

276 By using a background depleted in short-wavelength light,²⁷ we created substantial mela-
277 nopic contrast in our stimuli, albeit ~3.5x less than is available in rodent models with a shifted
278 long-wavelength cone.²⁵ We found that 100% contrast pulses were required to obtain a mea-
279 surable cortical response to melanopsin. The contrast response functions for both V1 fMRI

280 amplitude and persistent pupil constriction appeared to be in the linear range and rising even
281 at our maximum, 400% contrast level.

282 A characteristic property of the ipRGCs is their tonic firing to transient stimuli. Our model of
283 the evoked BOLD responses in V1 estimates the underlying duration of neural activity (Figure
284 S3). We observed an increasing duration of neural activity in response to melanopsin stimu-
285 lation across contrast levels, which was not seen in response to luminance stimulation (Figure
286 S4). We regard this result as tentative, however, principally because a similar, increasing du-
287 ration of neural response was seen for the “splatter” control modulation.

288 **A visual percept**

289 Consistent with the presence of a V1 neural response, we find that isolated melanopsin stim-
290 ulation is accompanied by a distinct visual percept. We viewed these stimuli over many hours
291 of experiments, and ourselves experienced the onset of the melanopsin spectral pulse as a
292 diffuse, minimal brightening of the visual field. The appearance was curiously unpleasant.

293 The diffuse, even blurry, property of the percept might be related to the broad receptive
294 fields of neurons driven by melanopsin stimulation,²⁸ consistent with the extensive dendritic
295 arbors of the ipRGCs.²⁹ In a prior study, subjects reported that lights appear brighter when
296 melanopsin contrast is added to the stimulation of the cone-based luminance channel.¹⁹ We
297 find a conceptually similar effect in our data, as subjects rated pulses of light flux (which contain
298 melanopic contrast) as brighter than pulses with cone contrast alone.

299 The most striking aspect of the percept evoked by the melanopsin pulse is that the brief
300 brightening is then followed by a fading of perception of the stimulus field, on occasion spread-
301 ing to involve the masked macular region of the stimulus. This was subjectively similar to
302 Troxler fading. This aspect was remarked upon by several of our naïve observers: “[the experi-
303 ence was] like blinding”; and “[the fade] to black that is the noise when your eyes are closed”; or
304 “kind of like if you got hit in the head really sharply . . . flashing lights and fade out.” (Table S2).
305 The melanopsin containing ipRGCs send recurrent axon collaterals to the inner plexiform layer
306 where they are positioned to modulate cone signals.³⁰ Consistent with this, melanopic con-
307 trast has been shown to attenuate cone-driven electroretinogram responses in the rodent over
308 minutes.²⁵ The prominent and rapid experience of fading for our melanopsin-directed stimulus
309 perhaps reflects the unopposed action of this attenuation mechanism.

310 Our data do not allow us to determine if one or more of these perceptual experiences arise

311 as a direct consequence of ipRGC signals arriving at visual cortex sites, or from the interaction
312 of melanopsin and cone signals at earlier points in the visual pathway.

313 **The challenge of photoreceptor isolation and the question of flicker**

314 Our conclusions depend upon the successful isolation of targeted photoreceptor channels.
315 Measurements and simulations indicate that the functional MRI results are unlikely to be ex-
316 plained by inadvertent cone contrast from known sources of biological variation (Figure S5).¹⁴
317 Nonetheless, we think it prudent to carry forward concern regarding inadvertent cone intru-
318 sion, and to search for additional means to exclude this possible influence. For example, in
319 the current study we examined in the functional MRI data whether there was a difference in
320 the time-course of response to luminance and melanopsin-directed stimuli, but did not find
321 convincing evidence of such. A time-course dissociation in the fMRI data would have provided
322 further support—similar to that obtained in the pupil data—that our stimuli drive distinct mech-
323 anisms. Different temporal profiles of stimulation may afford greater traction on this question in
324 future studies.

325 In our perceptual experiment, the melanopsin stimulus was reported to have a change in
326 hue. This was usually, but not universally, reported as a yellow-orange. In this experiment
327 we do not have available an estimate of the amount of reported color change that may be
328 attributable to imperfections in cone silencing. Consequently, we are unable to reject the pos-
329 sibility that small amounts of chromatic splatter produce this percept.

330 Our results are also subject to any systematic deviation of photoreceptor sensitivity from
331 that assumed in the design of our spectral modulations. One example model deviation is the
332 presence of “penumbral” cones that lie in the shadow of blood vessels, and thus receive the
333 stimulus spectrum after it has passed through the hemoglobin transmittance function. These
334 photoreceptors can be inadvertently stimulated by a melanopsin-directed modulation, produc-
335 ing a percept of the retinal blood vessels when the spectra are rapidly flickered (≥ 4 Hz).¹³
336 While it is possible to also silence the penumbral cones in the melanopsin stimulus,⁹ this
337 markedly reduces available contrast upon melanopsin (below 100%). We circumvented this
338 problem here by windowing the onset of the melanopsin stimulus with a gradual transition
339 (effectively 1 Hz) that removed the penumbral cone percept from our stimulus pulse.

340 We did not explicitly silence rods in our melanopsin-directed stimulus. Our background is
341 at light levels considered to be above rod intrusion, and we have previously demonstrated a

342 pupil response to melanopsin-directed modulation around a background an order of magni-
343 tude brighter,¹⁰ indicating that the melanopsin system responds at light levels well above rod
344 intrusion. In principle, we could further exclude the possibility of rod intrusion by examining a
345 flickering version of our melanopsin-directed stimulus. In such an experiment we would iden-
346 tify a flicker frequency at which rods could respond (if not saturated) but for which melanopsin
347 might not be expected to do so (e.g., 4-8 Hz). Finding no cortical response to the stimulus
348 would support the contention that the rods are saturated. In practice, this control experiment
349 faces two challenges. First, melanopsin may still respond within this frequency range.⁷ Sec-
350 ond, this stimulus may drive the penumbral cones, producing a percept of the blood vessels and
351 a cortical response.^{9,13} Modifying the stimulus to silence the penumbral cones would markedly
352 reduce available contrast on both the rods and melanopsin, defeating the purpose of the ex-
353 periment. Nonetheless, we attempted this control study and obtained uninformative results
354 (Figure S6). An important area for future investigation is the relationship between rod and
355 melanopsin signals in the transition between mesopic and photopic vision.

356 We note that these challenges attend our prior study of cortical responses to rapid mela-
357 nopsin flicker.⁹ In those experiments, penumbral-cone silent, sinusoidal melanopsin modula-
358 tions with 16% Michelson contrast were studied. For comparison to the stimuli used here, we
359 can express contrast as the peak of the sinusoid relative to the trough. This yields ~40% Weber
360 contrast. Given our finding here that roughly 100% Weber contrast was needed to evoke a V1
361 response, we now regard this prior study as not fully resolving the possibility that rapid modula-
362 tion of the ipRGCs drives a cortical response. The challenge of obtaining sufficient melanopsin
363 contrast while avoiding inadvertent stimulation of the penumbral cones is present as well in
364 studies of the perceptual detection of nominally cone-silent flicker.^{27,31}

365 **Conclusions**

366 Our results suggest that people can “see” with melanopsin. The high-contrast, melanopsin-
367 isolating spectral modulation we studied is a distinctly unnatural stimulus, but a valuable tool
368 for demonstrating the presence of a melanopic signal in the cortical visual pathway. Many of
369 our subjects found the melanopsin-directed stimulus to be unpleasant to view. We are curious
370 if variation in the perceptual or cortical response to this stimulus is related to the symptom of
371 photophobia.³² Under naturalistic conditions, it appears that melanopsin adjusts the sensitivity
372 of the cone pathways.²⁵ The interaction of melanopsin and cone signals in human vision is an

373 exciting avenue for investigation, particularly given recent findings of a role for melanopsin in
374 the coarse spatial coding of light intensity.²⁸

References

1. Andrew S, H BD. In: M B, editor. OSA Handbook of Optics, Ed 3. New York: McGraw-Hill; 2010. p. 11.11–11.104.
2. Dacey DM, Liao HW, Peterson BB, Robinson FR, Smith VC, Pokorny J, et al. Melanopsin-expressing ganglion cells in primate retina signal colour and irradiance and project to the LGN. *Nature*. 2005;433(7027):749–754.
3. Lucas RJ, Hattar S, Takao M, Berson DM, Foster RG, Yau KW. Diminished pupillary light reflex at high irradiances in melanopsin-knockout mice. *Science*. 2003 Jan;299(5604):245–7.
4. Gamlin PDR, McDougal DH, Pokorny J, Smith VC, Yau KW, Dacey DM. Human and macaque pupil responses driven by melanopsin-containing retinal ganglion cells. *Vision Res*. 2007 Mar;47(7):946–54.
5. Hattar S, Lucas RJ, Mrosovsky N, Thompson S, Douglas RH, Hankins MW, et al. Melanopsin and rod-cone photoreceptive systems account for all major accessory visual functions in mice. *Nature*. 2003 Jul;424(6944):76–81.
6. Nosedá R, Kainz V, Jakubowski M, Gooley JJ, Saper CB, Digre K, et al. A neural mechanism for exacerbation of headache by light. *Nat Neurosci*. 2010 Feb;13(2):239–45.
7. Do MTH, Kang SH, Xue T, Zhong H, Liao HW, Bergles DE, et al. Photon capture and signalling by melanopsin retinal ganglion cells. *Nature*. 2009;457(7227):281–287.
8. Davis KE, Eleftheriou CG, Allen AE, Procyk CA, Lucas RJ. Melanopsin-derived visual responses under light adapted conditions in the mouse dLGN. *PLoS One*. 2015;10(3):e0123424.
9. Spitschan M, Datta R, Stern AM, Brainard DH, Aguirre GK. Human visual cortex responses to rapid cone and melanopsin-directed flicker. *Journal of Neuroscience*. 2016;36(5):1471–1482.
10. Spitschan M, Jain S, Brainard DH, Aguirre GK. Opponent melanopsin and S-cone signals in the human pupillary light response. *Proceedings of the National Academy of Sciences*. 2014;111(43):15568–15572.

REFERENCES

REFERENCES

11. Benson NC, Butt OH, Brainard DH, Aguirre GK. Correction of distortion in flattened representations of the cortical surface allows prediction of V1-V3 functional organization from anatomy. *PLoS Comput Biol.* 2014;10(3):e1003538.
12. Boynton GM, Engel SA, Glover GH, Heeger DJ. Linear systems analysis of functional magnetic resonance imaging in human V1. *J Neurosci.* 1996 Jul;16(13):4207–21.
13. Spitschan M, Aguirre GK, Brainard DH. Selective stimulation of penumbral cones reveals perception in the shadow of retinal blood vessels. *PloS one.* 2015;10(4):e0124328.
14. Asano Y, Fairchild MD, Blondé L. Individual Colorimetric Observer Model. *PloS one.* 2016;11(2):e0145671.
15. Adelson EH. Saturation and adaptation in the rod system. *Vision research.* 1982;22(10):1299–1312.
16. Aguilar M, Stiles W. Saturation of the rod mechanism of the retina at high levels of stimulation. *Journal of Modern Optics.* 1954;1(1):59–65.
17. Hung SM, Milea D, Rukmini AV, Najjar RP, Tan JH, Viénot F, et al. Cerebral neural correlates of differential melanopic photic stimulation in humans. *NeuroImage.* 2017;146:763–769.
18. Tse PU, Baumgartner FJ, Greenlee MW. Event-related functional MRI of cortical activity evoked by microsaccades, small visually-guided saccades, and eyeblinks in human visual cortex. *Neuroimage.* 2010 Jan;49(1):805–16.
19. Brown TM, Tsujimura Si, Allen AE, Wynne J, Bedford R, Vickery G, et al. Melanopsin-based brightness discrimination in mice and humans. *Current Biology.* 2012;22(12):1134–1141.
20. Cole GR, Hine T, McIlhagga W. Detection mechanisms in L-, M-, and S-cone contrast space. *JOSA A.* 1993;10(1):38–51.
21. Chaparro A, Stromeyer CF 3rd, Huang EP, Kronauer RE, Eskew RT Jr. Colour is what the eye sees best. *Nature.* 1993 Jan;361(6410):348–50.

REFERENCES

REFERENCES

22. Zaidi FH, Hull JT, Peirson SN, Wulff K, Aeschbach D, Gooley JJ, et al. Short-wavelength light sensitivity of circadian, pupillary, and visual awareness in humans lacking an outer retina. *Current Biology*. 2007;17(24):2122–2128.
23. Brown TM, Gias C, Hatori M, Keding SR, Coffey PJ, Gigg J, et al. Melanopsin contributions to irradiance coding in the thalamo-cortical visual system. *PLoS Biol*. 2010;8(12):e1000558.
24. Schmidt TM, Chen SK, Hattar S. Intrinsically photosensitive retinal ganglion cells: many subtypes, diverse functions. *Trends Neurosci*. 2011 Nov;34(11):572–80.
25. Allen AE, Storchi R, Martial FP, Petersen RS, Montemurro MA, Brown TM, et al. Melanopsin-driven light adaptation in mouse vision. *Current biology*. 2014;24(21):2481–2490.
26. Winawer J, Witthoft N. Human V4 and ventral occipital retinotopic maps. *Visual neuroscience*. 2015;32:E020.
27. Cao D, Nicandro N, Barrionuevo PA. A five-primary photostimulator suitable for studying intrinsically photosensitive retinal ganglion cell functions in humans. *Journal of Vision*. 2015;15(1):27–27.
28. Allen AE, Storchi R, Martial FP, Bedford R, Lucas RJ. Melanopsin contributions to the representation of images in the early visual system. *Current Biology*. In press;.
29. Liao HW, Ren X, Peterson BB, Marshak DW, Yau KW, Gamlin PD, et al. Melanopsin-expressing ganglion cells on macaque and human retinas form two morphologically distinct populations. *J Comp Neurol*. 2016 Oct;524(14):2845–72.
30. Joo HR, Peterson BB, Dacey DM, Hattar S, Chen SK. Recurrent axon collaterals of intrinsically photosensitive retinal ganglion cells. *Visual neuroscience*. 2013;30(04):175–182.
31. Horiguchi H, Winawer J, Dougherty RF, Wandell BA. Human trichromacy revisited. *Proceedings of the National Academy of Sciences*. 2013;110(3):E260–E269.
32. Nosedá R, Kainz V, Jakubowski M, Gooley JJ, Saper CB, Digré K, et al. A neural mechanism for exacerbation of headache by light. *Nature neuroscience*. 2010;13(2):239–245.

1 **Online Methods**

2 **Pre-registration**

3 The experiments were the subject of pre-registration documents. Data collection followed the
4 pre-registration documents in regard to the number of subjects, extent of data collection, stim-
5 ulus generation, and exclusion criteria. In some cases addenda were submitted to the pre-
6 registration before data collection began, with the pre-registered protocol being that which
7 includes the modifications specified in these pre-data-collection addenda. In some cases the
8 analysis approach presented in this paper differs from that described in the pre-registered
9 protocol. Table S3 lists all pre-registration documents by experiment and deviations from the
10 registered protocols. Some deviations were detailed in addenda submitted after data collection
11 began, and these are also included as deviations in the table.

12 **Subjects and subject preparation**

13 Four subjects participated in the fMRI and pupillometry studies. All four participants are sci-
14 entific investigators and three are authors of this study (4 males, ages 27, 28, 32, 46). These
15 four participants choose to identify themselves by their initials. An additional 20 subjects, naïve
16 to the hypotheses of the study, participated in the perception experiment (9 men, 11 women,
17 mean age 27, range 20-33); their data have been assigned anonymous study identification
18 labels. All subjects were screened for normal color vision¹ and corrected acuity of 20/40 or
19 better as assessed by the Snellen chart at a 20 foot distance. All subjects were studied at
20 the University of Pennsylvania. The research was approved by the University of Pennsylvania
21 Institutional Review Board and conducted in accordance with the principles of the Declaration
22 of Helsinki. All subjects gave informed written consent.

23 Prior to fMRI scanning or perceptual rating, each subject underwent pharmacological dila-
24 tion of the right eye (1% tropicamide ophthalmic with 0.5% proparacaine as a local anesthetic
25 agent).

26 **Visual stimuli**

27 We used the method of silent substitution with a digital light synthesis engine (OneLight Spec-
28 tra) to stimulate targeted photoreceptors. Our device produces stimulus spectra as mixtures

29 of 56 independent, ~16 nm full-width half-max primaries under digital control, and can modu-
30 late between these spectra at 256 Hz. Details regarding the device, stimulus generation, and
31 estimates of precision have been previously reported.²⁻⁴

32 Our estimates of photoreceptor spectral sensitivities were as previously described,³ fol-
33 lowing the CIE physiological cone fundamentals.⁵ They account for the size of the visual field
34 (64°), subject age, and the pupil size, which we assumed to be 8 mm in diameter under phar-
35 macologic dilation.

36 Separate background and modulation spectra were identified to maximize available con-
37 trast on melanopsin and the combined stimulation of the L, M, and S cones. First, “mid-
38 background settings were selected so as to maximize available melanopsin (or LMS) Michelson
39 contrast for modulations symmetric around this background. Then, a 66.66% modulation was
40 found. The negative ‘arm’ of this modulation served as the experimental background, and the
41 positive ‘arm’ of this modulation represented the maximal, 400% contrast pulse. An additional
42 constraint sought to minimize the difference in calculated chromaticity of the backgrounds of
43 the LMS and melanopsin stimuli (Figures 1 and S1). The background for the LMS, Mel, and
44 Splatter modulations were all nominally rod-saturating (100-200 cd/m²; >3.3 log sc td). The
45 modulations did not explicitly silence penumbral cones.³

46 We elected not to perform psychophysical nulling of our stimuli for two reasons. First, in
47 an earlier study² we found that the test-retest reliability of nulling values produced by was
48 not high. We estimated that stimulus adjustment for individual subjects was more likely to
49 worsen photoreceptor silencing than to improve it. Second, we found that allowing for stimulus
50 adjustment would reduce the available gamut in our modulations, with the consequence of a
51 substantial reduction in available contrast on melanopsin.

52 We measured the melanopsin 400% background and stimulation spectra for a reference
53 observer (32 years) before and after each scanning session for each subject during our ini-
54 tial fMRI experiment (described as Experiment 1 below). We calculated the average post-
55 receptor contrast for each of these 8 spectra (4 subjects x 2 measurements) with respect to
56 the cone fundamentals assumed for the reference observer. From these measurements, we
57 derived 8 sets of post-receptor contrast values for LMS, L-M, and S-[L+M]. We then took the
58 sign preserved absolute maximum value across each of the sets of 8 measurements. The re-
59 sulting post-receptor contrast values [%] were LMS: +2.173; L-M: +0.877; S-[L+M]: -10.451.
60 Converted to cone contrast values [%] these were L: +3.050; M: +1.296; S: -8.278. We term

61 this set of cone contrasts the 1x splatter control modulation. When presented to individual
62 observers, the splatter control modulation was tailored to the age of the individual observers,
63 such that even though the spectra seen by the observers would be different, they would all
64 see a modulation with the nominal contrast values above, calculated using their age-corrected
65 cone fundamentals.

66 The stimulus was viewed within an MRI compatible eye piece that provided a circular, uni-
67 form field of 64° diameter. The central 5° diameter was obscured. Subjects were asked to
68 maintain fixation in the center of this obscured region to avoid stimulation within the macula,
69 where spatial variation in macular pigment could alter the spectral properties of the stimulus.

70 Three-second pulses of spectral change were presented during individual trials of 16 s
71 duration. During each trial, a transition from the background to the stimulation spectrum would
72 occur starting at either 0, 1, or 2 seconds after trial onset (randomized uniformly across trials);
73 this jitter was designed to reduce the ability of the subject to anticipate the moment of stimulus
74 onset and to render trial timing asynchronous with respect to BOLD fMRI image acquisition.
75 The transition from the background to the modulation spectrum, and the return to background,
76 was subjected to a 500 ms half-cosine window. This resulted in a slew rate lower than that we
77 found previously to produce a Purkinje tree percept due to stimulation of L and M cones that
78 are shadowed by retinal blood vessels.³

79 **Simulation of biological variability causing inadvertent cone contrast**

80 To address the amount of inadvertent stimulation of the L, M and S cones due to biological
81 variability not captured by the CIE model for the cone fundamentals (Figure S5), we performed
82 simulations of colorimetric observers, assuming variability in the following eight parameters:
83 lens density, macular pigment density; L cone photopigment density, M cone photopigment
84 density, S cone photopigment density; and the peak absorbance λ_{max} of the L, M and S cone
85 photopigments. Using previously published estimates of the standard deviations in those pa-
86 rameters⁶, we randomly sampled independently from normal distributions with those SDs. The
87 SDs were $\pm 18.7\%$ deviation in lens density, $\pm 25\%$ in macular pigment density; $\pm 9\%$ devia-
88 tion in L cone density, $\pm 9\%$ deviation in M cone density, $\pm 7.4\%$ deviation in S cone density;
89 and ± 2 nm, ± 1.5 nm and ± 1.3 nm in λ_{max} for L, M and S cones respectively. Note that the
90 variation in lens density was taken around the age-appropriate mean density for each subject.
91 We performed this resampling 1,000 times, generating 1,000 sets of spectral sensitivities. This

92 was done for the four observers from the fMRI studies (Figure S5) and the twenty observers
93 from the perceptual studies (Figure S11).

94 We present plots of the L, M, and S cone contrasts after transformation to a post-receptoral
95 opponent representation assuming mechanism sensitivities to cone contrast for luminance,
96 red-green, and blue-yellow mechanisms of $[0.5 \ 0.5 \ 0]$, $[0.5 \ -0.5 \ 0]$, and $[-0.5 \ -0.5 \ 1]$ respec-
97 tively. This transformation corresponds to the DKL opponent color space representation⁷ when
98 the background produces equal excitations in the L, M and S cones, for the case in which the
99 L and M cone spectral sensitivities are scaled so that they sum to produce the luminous ef-
100 ficiency curve. We regarded this as a reasonable choice of reference conditions to define
101 the transformation, as it leads to intuitively straightforward properties of the assumed post-
102 receptoral mechanisms. We note that for other backgrounds, this transformation will describe
103 the opponent mechanism responses to the extent that those responses are the same for mod-
104 ulations seen against different backgrounds, when the LMS cone contrasts of the modulations
105 are matched across backgrounds.

106 **Design of MRI experiments**

107 Each of the four primary subjects participated in six MRI experiments (except for subject ASO
108 who was unavailable to participate in the final, sixth experiment). The first two experiments
109 presented pulses of either 400% melanopsin contrast only (Experiment 1) or 400% LMS con-
110 trast only (Experiment 2). Three experiments presented intermixed trials of different intensity
111 of either “splatter” cone contrast (Experiment 3), melanopsin contrast (Experiment 4), or LMS
112 contrast (Experiment 5). The final experiment (described in Figure S6) presented blocks of
113 flickering L–M and melanopsin / rod modulations under scotopic and photopic conditions. Dur-
114 ing Experiments 1, 2, 3, and 6, the left eye was covered with an opaque patch. During Ex-
115 periments 4 and 5 the left eye was uncovered and monitored with an infrared video camera
116 (described below).

117 Each experimental session was approximately two hours. A given scanning session ex-
118 amined a single stimulus type (e.g., LMS, melanopsin, or splatter). The subject maintained
119 adaptation to the background spectrum between trials and scan runs. Prior to each fMRI
120 session, subjects underwent monocular dark adaptation for 20 minutes by wearing swimming
121 goggles with the right eye obscured. Once in the scanner, the right eye was adapted for at
122 least five minutes to the stimulus background prior to the start of functional scanning.

123 Experiments 3, 4 and 5 sought to measure the contrast response function (CRF) that re-
124 lated stimulus contrast to BOLD fMRI response. A set of stimuli of varying contrasts were
125 presented in an intermixed order during a given scan. The LMS and melanopsin CRF stud-
126 ies presented 5, logarithmically spaced contrast levels (25, 50, 100, 200, and 400% contrast);
127 the splatter CRF study presented 4 levels ($\frac{1}{4}x$, $\frac{1}{2}x$, $1x$, $2x$). The $2x$ stimulus was in fact $1.95x$
128 due to limitations in device gamut; we adopt the technically inaccurate label for ease of de-
129 scription and interpretation. Ordering of these trial types within and across scans followed a
130 pseudo-random, counter-balanced order.⁸

131 Functional MRI data collection took place during individual scans of 336 s duration. With
132 the exception of Experiment 6, each scan run presented 21, 16 s trials; Experiment 6 presented
133 blocks of stimulation and is described in Figure S6. Eighteen of the trials presented a spectral
134 pulse. Three randomly selected trials presented an “attention event” instead of a stimulus
135 pulse, during which the stimulus field dimmed for 500 ms. The subject was asked to press a
136 button on a response pad when these dimming events occurred. Between 9 and 12 scan runs
137 were collected for each subject for each experiment.

138 **MRI data acquisition and initial processing**

139 MRI scanning parameters made use of the Human Connectome Project LifeSpan protocol
140 (VD13D) implemented on a 3-Tesla Siemens Prisma with a 64-channel Siemens head coil. A
141 T1-weighted, 3D, magnetization-prepared rapid gradient-echo (MPRAGE) image was acquired
142 for each subject in axial orientation with 0.8 mm isotropic voxels, repetition time (TR)=2.4
143 s, echo time (TE)=2.22 ms, inversion time (TI)=1000 ms, field of view (FoV)=256 mm, flip
144 angle=8°. BOLD fMRI data were obtained over 72 axial slices with 2 mm isotropic voxels with
145 multi-band=8, TR=800 ms, TE=37 ms, FOV=208 mm, flip angle=52°. Head motion was mini-
146 mized with foam padding. Although continuous pulse-oximetry was recorded, this physiologic
147 measurement was not used in the fMRI data analysis.

148 The FreeSurfer (v5.3) toolkit (<http://surfer.nmr.mgh.harvard.edu/>)⁹⁻¹² was used to
149 process anatomical MPRAGE images to construct inflated brain surfaces and register data
150 from across subjects for surface visualization. Briefly, this processing includes spatial in-
151 homogeneity correction, non-linear noise-reduction, skull-stripping,¹³ subcortical segmenta-
152 tion,^{14,15} intensity normalization,¹⁶ surface generation,^{9,10,17} topology correction,^{18,19} surface
153 inflation,¹⁰ and registration to a spherical atlas.¹¹

154 Raw echo-planar volumetric data were motion corrected using the FMRIB Software Library
155 (FSL) toolkit (<http://fsl.fmrib.ox.ac.uk/fsl/>). Motion corrected functional volumes were
156 co-registered to subject-specific anatomy in Freesurfer using FSL-FLIRT with 6 degrees-of-
157 freedom under a FreeSurfer wrapper (`bregister`).

158 **BOLD fMRI time-series analysis**

159 The pipeline for the analysis of the BOLD fMRI time series is available on GitHub
160 (<https://github.com/gkaguirrelab/MRklar/releases/tag/v1.0.0>). Noise regressors
161 were derived from the left, right, third, and fourth ventricles, as well as white matter, brain
162 stem white matter, and non-brain tissue. Binary masks of these regions were initially identi-
163 fied in a Freesurfer anatomical segmentation volume (`aseg.mgz`). After co-registering to the
164 functional volume, these regions were eroded by two voxels (for the white matter mask) or a
165 single voxel (for all other regions) to avoid partial volume contamination from grey matter. The
166 first five principal components of the time-series data across all voxels in these regions were
167 then used as regressors. The signal from white matter local to each voxel was obtained and
168 regressed. To obtain the local white matter signal for each voxel, the mean time series of all
169 white matter voxels within a 15 mm radius sphere was regressed from the time series of the
170 voxel found at the center of the sphere. This local white matter procedure was modeled after
171 the ANATICOR pipeline in AFNI.²⁰ Twenty-four motion regressors were derived from the initial
172 six parameters that result from motion correction.²¹ The effects of these nuisance covariates
173 were removed from the time-series data by regression. Finally, the time-series was subjected
174 to a high-pass Butterworth filter with a cut-off of 0.01 Hz.

175 We conducted whole brain (cortical surface) analysis of the data from Experiments 1 (400%
176 melanopsin only) and 2 (400% LMS only). The time-series data from each voxel for each
177 subject was projected to hemisphere-symmetric cortical surface atlas (`fsaverage-sym`) and
178 smoothed on the cortical surface using a 5 mm full-width at half-maximum Gaussian kernel.
179 An approximation to a Fourier basis set analysis was conducted on the time-series data at each
180 cortical point for each of the k scan runs using the FSL FEAT and FOBS routines, modeling the
181 14 s period following each stimulus event with a set of 14 “harmonics”, which were sinusoids
182 that varied in frequency from half a cycle per period to 14 cycles per period. The p -value as-
183 sociated with the F-statistic for this model was obtained at each vertex. For each subject and
184 hemisphere (at each cortical point), the set of p -values across the k scan runs were used to

185 calculate a χ^2 -value with $2k$ degrees of freedom using Fisher's method. The map of p -values
186 corresponding to the χ^2 map from each subject and hemisphere were combined again using
187 Fisher's method, and the resulting maps of χ^2 -values were used to illustrate the evoked stimu-
188 lus effect shown in Figure 2a, b. These maps were thresholded at a value of χ^2 (16 df)=61.4.
189 This corresponds to a Bonferroni corrected, map-wise $p = 0.05$ threshold after accounting for
190 the number of vertices in the group map (and disregarding map spatial smoothness).

191 The primary analyses of the study were conducted within a V1 region of interest. A cor-
192 tical surface atlas²² was used to define a patch of V1 cortex corresponding to the radial ec-
193 centricity range of 5–25°. For each subject, the average, post-processed signal within this
194 region (and across the two hemispheres) was obtained for each scan run in each experi-
195 ment. The regional time-series data were analyzed within a non-linear temporal fitting engine
196 (<https://github.com/gkaguirrelab/temporalFittingEngine>).

197 Experiments 1-5 included intermittent attention events. Subjects performed well on this
198 detection task. Collapsing performance across subjects and experiments, there were 0 false
199 alarm responses during the 3,816 stimulus trials, and 11 misses during the 636 attention trials.
200 We treated the attention events as an impulse input to the visual system and derived the
201 ensuing response function for each subject across the set of roughly 50 scan runs using a
202 Fourier basis set approach.²³ The 16 s following the onset of each event was modeled with
203 8 harmonics (temporal resolution of 1 Hz). The fit to the evoked response was averaged
204 across scan runs to obtain an estimate of the hemodynamic response function (HRF) for each
205 subject (Figure S3). As the timing of attention events was asynchronous with respect to image
206 acquisition (TRs), this approach provided an accurate estimate of the underlying response not
207 available from a simple averaging of the time-series data itself across trials.

208 The timing of stimulus events was also asynchronous with respect to image acquisition.
209 Therefore, the same Fourier basis set approach was used to obtain estimates of the evoked
210 BOLD fMRI response to the various spectral pulses studied in Experiments 1-5 (Figures 2d, 2e,
211 S2). The average evoked response for each stimulus type for each subject was then modeled
212 with a two-parameter model (Figure S2b). The first parameter controlled the duration of a step-
213 function of neural activity that was then convolved by the HRF for the subject. The resulting
214 shape of BOLD fMRI response was normalized to have unit amplitude, and then subjected
215 to a gain parameter. The best fitting parameters (in the least-squares sense) were found by
216 non-linear search (`fmincon`).

217 We observed that our subjects differed in the overall amplitude of their BOLD fMRI HRF.
218 We obtained the set of peak amplitude HRF values for each subject, and then divided each
219 value by the mean of the values across subjects. We treated the result as a “subject scaler”
220 that was used to normalize other measurements of response amplitude from each subject to
221 remove this individual difference.

222 **Eye and pupil tracking**

223 Infra-red (IR) video eye-tracking was performed during Experiments 4 and 5. The LiveTrack
224 AV MR-compatible eye tracking camera (Cambridge Research Systems, Rochester, UK) was
225 used to record video from the left eye of each subject at either 60 Hz or 30 Hz (the lower frame
226 rate was used in the Mel CRF studies for ASO and GKA, and in the LMS CRF study for ASO).
227 The camera was attached to the 64-channel head coil using a custom mount, and positioned
228 10-15 cm away from the left eye of the subject. The camera and head coil were draped in
229 black felt to minimize scattering of light to the left eye from the eyepiece over the right eye.
230 Consistent with the minimization of scattered light and room light, subjects generally reported
231 binocular suppression of the left eye during these experiments.

232 A live video feed from the system was used to monitor subject alertness and head motion
233 during scanning. The system recorded the position of the IR glint on the tear film and the size
234 and position of an ellipse fit to the outline of the pupil in each frame, and from this derived
235 pupil size and eye position. We found that the automated ellipse fitting was unstable in the
236 vertical dimension. For this reason, we report here the pupil size derived from the horizontal
237 width of the fitted ellipse, and eye position in the horizontal plane only. The timing of data
238 collection was synced with MRI scan acquisition and stimulus presentation using an analog
239 signal (TTL) sent by the scanner at the start of the scan and at the time of each image repetition
240 (TR). Absolute pupil size was determined by calibrating the camera against targets of known
241 dimension following each scan session.

242 The analysis pipeline for the pupil and eye position data is available on GitHub
243 (<https://github.com/gkaguirrelab/pupilMelanopsinMRIAnalysis>). First, blinks were
244 identified as timepoints during which the glint was not visible. The pupil size and position
245 measurements were set to NaN in the 50 ms before and after each blink. The pupil size
246 vectors were then subjected to a 0.025 Hz high-pass filter. A 13 s period of pupil response
247 following the onset of every trial was extracted, expressed in percent change units, and set

248 to have a value of zero during the first 100 ms following the onset of the stimulus. The
249 median response across trials for each stimulus type for each subject was obtained (Figure
250 S8). Each median response was then fit with a six-parameter, three-component pupil tem-
251 poral model (Figure S9) using a non-linear search (fmincon) within a temporal fitting engine
252 (<https://github.com/gkaguirrelab/temporalFittingEngine>).

253 We observed that our subjects differed in the overall amplitude of their pupil response. For
254 each subject, we obtained the total area of pupil response (% change x seconds) across all
255 stimulus types (mel and LMS pulses of every contrast level). We divided each value by the
256 mean of the set of values across subjects. We treated the result as a “subject scaler” that
257 was used to normalize measurements of response amplitude from each subject to remove this
258 individual difference.

259 **Perceptual rating experiment**

260 Perceptual ratings were obtained from experimentally naïve subjects using the same stimulus
261 presentation apparatus as was used in the fMRI experiments. Subjects were positioned in a
262 chin rest in a darkened room and observed stimuli with their pharmacologically dilated right
263 eye. The experiment was composed of several periods. In each period, the subject would
264 first adapt to a stimulus background, and then view spectral pulses of a particular stimulus
265 type (light flux, LMS, or melanopsin). Three initial “exposure” periods were used to familiarize
266 subjects with the procedure and the perceptual range of the stimuli. Each exposure consisted
267 of 1 min of adaptation to the background, followed by presentation of 3 spectral pulse trials
268 of a given type. Subjects were asked only to observe the stimuli. Following the exposure
269 periods, the subject participated in six “rating” periods. Each rating period consisted of a 5
270 min adaptation to a background, followed by the presentation of 9 spectral pulse trials of a
271 given type. Before each trial, the subject was read a description of a perceptual property that
272 they were to rate for the upcoming stimulus trial. Following presentation of the stimulus pulse,
273 the subject was prompted for their rating on a scale of 1 to 7. The subject could ask for the
274 description and pulse to be repeated one additional time prior to providing a rating. The subject
275 was asked to rate a different perceptual property for each of the 9 trials in a given rating period.
276 Rating periods for light flux, LMS, and melanopsin stimuli were each conducted twice, with
277 subjects randomized to follow one of two trial orders:

278 i. light flux, melanopsin, LMS, light flux, melanopsin, LMS

279 ii. light flux, LMS, melanopsin, light flux, LMS, melanopsin

280 The nine perceptual properties were defined by pairs of antonyms (e.g., cool–warm) that
281 defined the extreme ratings of 1 and 7. Subjects were instructed to fixate the center of the
282 stimulus field and report the appearance of the light pulse in visual periphery, doing their best
283 to ignore any percept within or adjacent to the obscured macular region.

284 For the perceptual rating experiment, our photoreceptor spectral sensitivity estimates as-
285 sumed a (27.5°) field for generating the receptor-isolating modulations while the observed field
286 was in fact (64°) as in the fMRI experiments. This led to numerical but insignificant differences
287 in the estimate for the macular pigment density. In the contrast and splatter calculations for this
288 experiment, we assumed the 64° in our estimates for the spectral sensitivities.

289 The first two dimensions of the principal components analysis of the perceptual rating data
290 were used to describe the results as the addition of further dimensions was found to reduce
291 cross-validated categorization accuracy.

292 **Spectrum seeking to improve stimulus control**

293 The stimuli used in the perceptual study were subjected to an additional refinement prior
294 to each data collection session, designed to further reduce inadvertent cone contrast in the
295 melanopsin-directed stimulus. An adaptive spectrum-correcting procedure addressed uncer-
296 tainty in our device calibration due to instrumental drift and small failures of primary additivity.
297 This procedure adjusted the mirror settings in our digital light synthesis engine so as to match
298 the nominal, receptor-isolating spectra. This procedure was performed for the age-adjusted
299 stimuli of all subjects in the perceptual rating experiment.

300 We started with a pair of primary values designed to yield a certain contrast: The back-
301 ground primary values P_{BG} and the modulation primary values P_{Mod} . The spectral calibration
302 procedure of the light synthesis engine determines the primary matrix M , which, when mul-
303 tiplied with the primary values and added to the dark spectrum spd_{dark} , yields the predicted
304 target spectra $spd_{BG; target}$ and $spd_{Mod; target}$. Contrast properties of the stimulus are defined
305 with respect to these two spectra.

306 During a validation, we gamma-correct the linear primaries values, P using our device cal-
307 ibration model. This yields the pair of settings S_{BG} and S_{Mod} . These are then provided to the

308 light engine and spectral measurements $spd_{BG; val}$ and $spd_{Mod; val}$ are obtained. Due to impre-
309 cision in the stimulus control, $spd_{BG; target}$ and $spd_{BG; val}$, and $spd_{Mod; target}$ and $spd_{Mod; val}$,
310 are different.

311 The goal of the adaptive procedure is to find terms ΔP_{BG} and ΔP_{Mod} which correct the
312 primary values. To do this, we do the following ($i \in 1 \dots N$, where typically $N = 10$).

- 313 i. Gamma correct: $P_{i; BG} \rightarrow S_{i; BG}$ and $P_{i; Mod} \rightarrow S_{i; Mod}$
- 314 ii. Obtain target spectra: $P_{1; BG} \rightarrow spd_{BG; target}$ and $P_{1; Mod} \rightarrow spd_{Mod; target}$
- 315 iii. Measure $spd_{i; BG; val}$ and $spd_{i; Mod; val}$
- 316 iv. Calculate the spectral difference between target and validated spectra in the i -th iteration:
317 $\Delta spd_{i; BG} = spd_{BG; target} - spd_{i; BG; val}$ and $\Delta spd_{i; Mod} = spd_{Mod; target} - spd_{i; Mod; val}$.
- 318 v. Obtain $\Delta P_{i; BG}$ and $\Delta P_{i; Mod}$ corresponding to the spectral differences using our calibra-
319 tion model that maps spectra back to device coordinates.
- 320 vi. Update the primary values for the next iteration: $P_{i+1; BG} = P_{i; BG} + \lambda \Delta P_{i; BG}$ and
321 $P_{i+1; Mod} = P_{i; Mod} + \lambda \Delta P_{i; Mod}$, where $\lambda = 0.8$ is the learning rate.

322 We find that this spectrum-correction procedure reliably reduces inadvertent cone stimula-
323 tion due to uncertainty in device control.

324 Data and code availability

325 All raw data are available as packaged and MD5-hashed archives as well as tables detailing
326 the biological variability on FigShare (<https://figshare.com/s/0baea6ed50758abbabf4>).

327 All code is available in public GitHub repositories. Un-thresholded statistical
328 maps from Experiments 1 and 2 for each subject are available from NeuroVault
329 (<http://neurovault.org/collections/2459/>).

References

1. Ishihara S. Tests for Colour-Blindness. Tokyo: Kanehara Shuppen Company, Ltd.; 1977.
2. Spitschan M, Datta R, Stern AM, Brainard DH, Aguirre GK. Human visual cortex responses to rapid cone and melanopsin-directed flicker. *Journal of Neuroscience*. 2016;36(5):1471–1482.
3. Spitschan M, Aguirre GK, Brainard DH. Selective stimulation of penumbral cones reveals perception in the shadow of retinal blood vessels. *PloS one*. 2015;10(4):e0124328.
4. Spitschan M, Jain S, Brainard DH, Aguirre GK. Opponent melanopsin and S-cone signals in the human pupillary light response. *Proceedings of the National Academy of Sciences*. 2014;111(43):15568–15572.
5. CIE. Fundamental Chromaticity Diagram with Physiological Axes - Part 1. Commission Internationale de l'Eclairage; 2006. 170-1.
6. Asano Y, Fairchild MD, Blondé L. Individual Colorimetric Observer Model. *PloS one*. 2016;11(2):e0145671.
7. Brainard D. Cone contrast and opponent modulation color spaces. *Human color vision*. 1996;2:563–579.
8. Aguirre GK, Mattar MG, Magis-Weinberg L. de Bruijn cycles for neural decoding. *NeuroImage*. 2011;56(3):1293–1300.
9. Dale AM, Fischl B, Sereno MI. Cortical surface-based analysis: I. Segmentation and surface reconstruction. *Neuroimage*. 1999;9(2):179–194.
10. Fischl B, Sereno MI, Dale AM. Cortical surface-based analysis: II: inflation, flattening, and a surface-based coordinate system. *Neuroimage*. 1999;9(2):195–207.
11. Fischl B, Sereno MI, Tootell RB, Dale AM, et al. High-resolution intersubject averaging and a coordinate system for the cortical surface. *Human brain mapping*. 1999;8(4):272–284.
12. Fischl B, Dale AM. Measuring the thickness of the human cerebral cortex from magnetic resonance images. *Proceedings of the National Academy of Sciences*. 2000;97(20):11050–11055.

REFERENCES

REFERENCES

13. Ségonne F, Dale A, Busa E, Glessner M, Salat D, Hahn H, et al. A hybrid approach to the skull stripping problem in MRI. *Neuroimage*. 2004;22(3):1060–1075.
14. Fischl B, van der Kouwe A, Destrieux C, Halgren E, Ségonne F, Salat DH, et al. Automatically parcellating the human cerebral cortex. *Cerebral cortex*. 2004;14(1):11–22.
15. Fischl B, Salat DH, Busa E, Albert M, Dieterich M, Haselgrove C, et al. Whole brain segmentation: automated labeling of neuroanatomical structures in the human brain. *Neuron*. 2002;33(3):341–355.
16. Sled JG, Zijdenbos AP, Evans AC. A nonparametric method for automatic correction of intensity nonuniformity in MRI data. *IEEE transactions on medical imaging*. 1998;17(1):87–97.
17. Dale AM, Sereno MI. Improved localization of cortical activity by combining EEG and MEG with MRI cortical surface reconstruction: a linear approach. *Journal of cognitive neuroscience*. 1993;5(2):162–176.
18. Fischl B, Liu A, Dale AM. Automated manifold surgery: constructing geometrically accurate and topologically correct models of the human cerebral cortex. *IEEE transactions on medical imaging*. 2001;20(1):70–80.
19. Ségonne F, Pacheco J, Fischl B. Geometrically accurate topology-correction of cortical surfaces using nonseparating loops. *IEEE transactions on medical imaging*. 2007;26(4):518–529.
20. Jo HJ, Gotts SJ, Reynolds RC, Bandettini PA, Martin A, Cox RW, et al. Effective preprocessing procedures virtually eliminate distance-dependent motion artifacts in resting state fMRI. *Journal of applied mathematics*. 2013;2013.
21. Friston KJ, Williams S, Howard R, Frackowiak RS, Turner R. Movement-related effects in fMRI time-series. *Magnetic resonance in medicine*. 1996;35(3):346–355.
22. Benson NC, Butt OH, Brainard DH, Aguirre GK. Correction of distortion in flattened representations of the cortical surface allows prediction of V1-V3 functional organization from anatomy. *PLoS Comput Biol*. 2014;10(3):e1003538.
23. Aguirre GK, Zarahn E, D’Esposito M. The variability of human, BOLD hemodynamic responses. *Neuroimage*. 1998;8(4):360–369.

Supplementary Material

List of Figures

- Figure S1: Spectra and chroma of all stimuli (related to Figure 1)
- Figure S2: Additional BOLD fMRI time-series and model fits (related to Figure 2)
- Figure S3: HRFs and evoked response model (related to Figure 2)
- Figure S4: Amplitude and duration of response in V1 by stimulus contrast (related to Figure 3)
- Figure S5: Inadvertent cone contrast in the fMRI stimuli (related to Figure 3)
- Figure S6: An unsuccessful control experiment (related to Figure 3)
- Figure S7: Variation in horizontal gaze position with stimulation (related to Figure 4)
- Figure S8: Individual subject pupil responses (related to Figure 4)
- Figure S9: Pupil temporal model (related to Figure 4)
- Figure S10: Temporal pupil model parameters by contrast (related to Figure 4)
- Figure S11: Inadvertent cone contrast in the perceptual stimuli (related to Figure 5)
- Table S1: Across-subject ratings of nine perceptual qualities for 400% contrast pulses of the three stimulus types
- Table S2: Free-form descriptions of the pulsed stimuli
- Table S3: Pre-registered experiments and protocol deviations

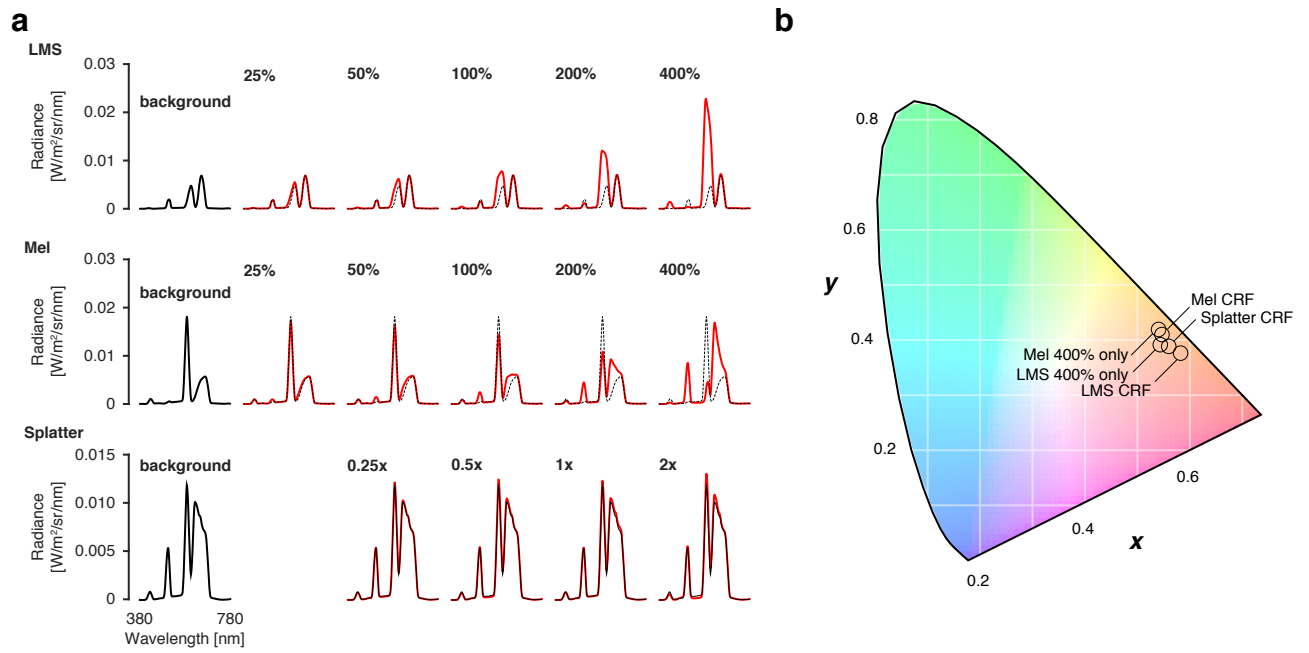


Figure S1: Spectra and chroma of all stimuli (related to Figure 1). (a) The stimulation spectra (red) for each contrast level in comparison to the background spectrum (black) for the LMS, melanopsin, and splatter stimuli. (b) The calculated CIE 1931 chromaticity¹ for all stimulus backgrounds. Experiments that presented stimuli of different contrast levels are indicated with “CRF” (Contrast Response Function).

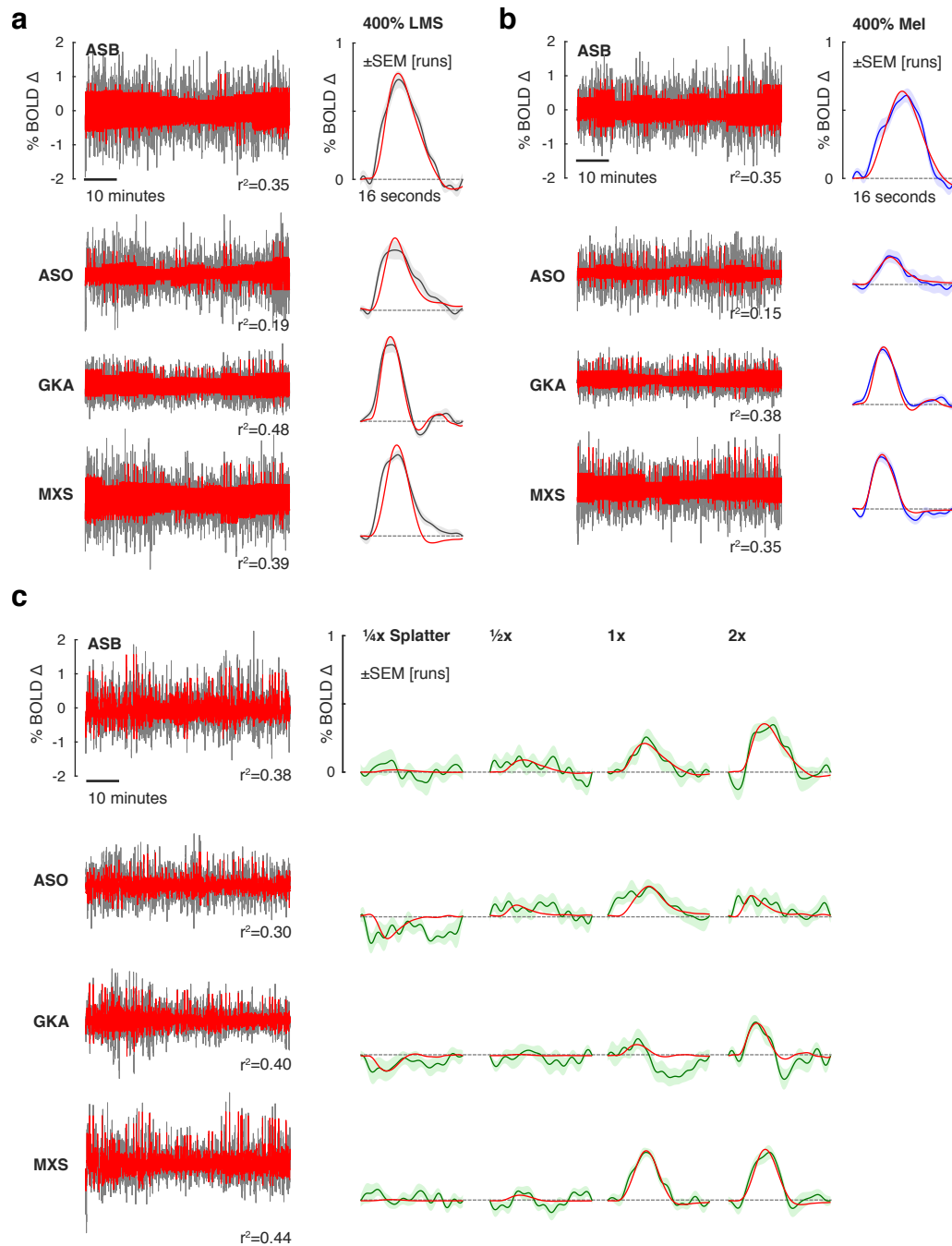


Figure S2: Additional BOLD fMRI time-series and model fits (related to Figure 2). (a) V1 responses to 400% LMS stimulation. Our initial study to explore broad cortical responses presented only trials with 400% stimulus contrast. *Left* The BOLD fMRI time-series data from the area V1 region for each subject (black), following pre-processing to remove nuisance effects. A Fourier basis set modeled (red) the mean evoked response to each contrast level during each run with the r^2 values of the model fit indicated. *Right* The evoked responses for each subject to the 400% LMS stimuli (black), and SEM of the response across the 9-10 scanning runs performed in each subject (shaded region). The responses were fit by a model (red) that convolved a step function of neural activity by the hemodynamic response function measured for each subject. (b) The corresponding responses within the V1 region to melanopsin stimulation of 400% contrast. (c) The corresponding responses within the V1 region to the “splatter” modulation, with contrast varying from one-quarter to two-times the estimated cone splatter contrast arising from device imprecision (see Online Methods, Figure S5).

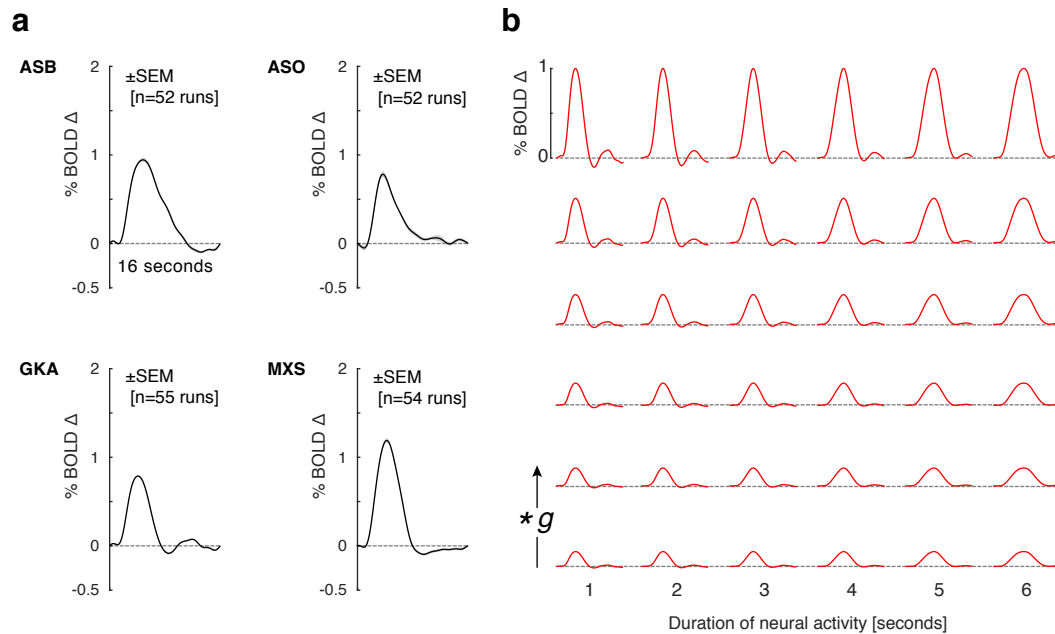


Figure S3: HRFs and evoked response model (related to Figure 2). (a) In all experiments, 14% of stimulus trials were randomly replaced with an attention event, during which the stimulus dimmed for 500 ms and in response to which the subject was to press a button on a response pad. The same response events occurred in each of the >50, 336 second scan runs for each subject across all experimental conditions. The BOLD fMRI response evoked within the studied V1 region in response to the attention events was estimated using a Fourier basis set for each run for each subject. The 16 s that followed each event was modeled with 8 harmonics, providing a temporal resolution of 1 Hz. The average response across runs (black) for each subject (expressed in units of percent BOLD signal change) was taken to be an estimate of the hemodynamic impulse response for that subject and was used in modeling of fMRI responses to other stimulation conditions for that subject. The SEM of the response across runs (shaded gray) is in most cases smaller than the plot line. (b) Shown are how the predicted BOLD fMRI responses for subject GKA vary with inferred duration of neural activity (across each row) and amplitude of BOLD fMRI response (each row shows a different value of g). The model varied the duration of a step function of neural activity that was then convolved with the HRF for that subject and subjected to multiplicative scaling ($*g$) to best fit the evoked response. The fits provided by this model are shown in Figure 2 and Figure S2, and the amplitude and duration parameters derived from fitting are the subject of Figures 3 and S4.

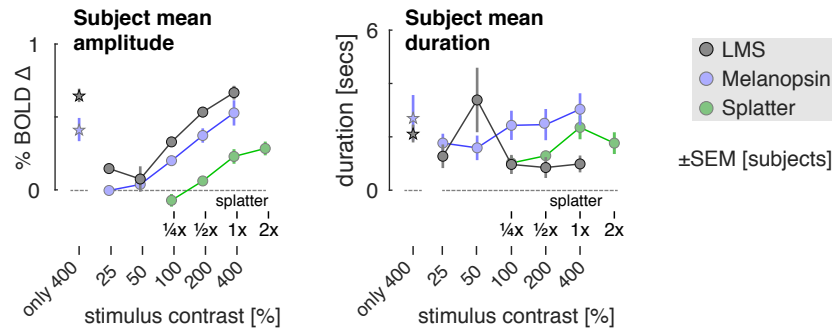


Figure S4: Amplitude and duration of response in V1 by stimulus contrast (related to Figure 3). (a) The mean amplitude of evoked response with the V1 region across subjects for each contrast level is shown for the LMS (gray), melanopsin (cyan), and “splatter” (green) stimulus conditions. The open star symbols are the amplitude measurements obtained in the initial, 400% contrast only LMS and melanopsin studies. The 1x splatter condition presented cone contrast equal to the maximum inadvertent contrast measured in validated spectra in the melanopsin and LMS experiments. (b) The mean modeled duration across subjects of underlying neural activity within the V1 region is shown for the three stimulus conditions.

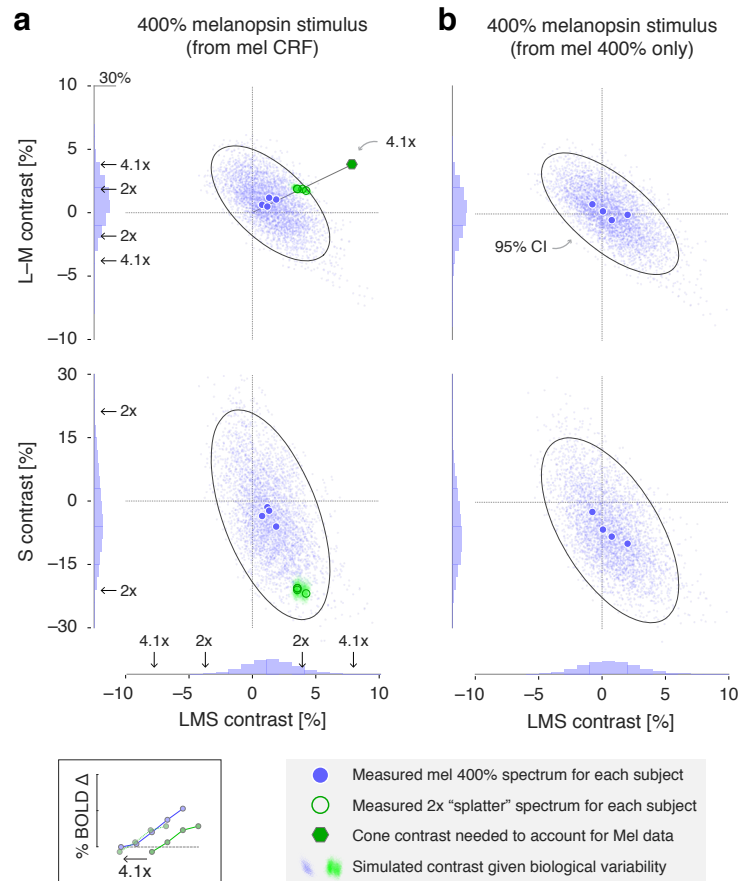


Figure S5: Inadvertent cone contrast in the fMRI stimuli (related to Figure 3). (a) Due to biological variability and inevitable imperfections in device control, a nominally cone silent modulation will produce inadvertent contrast upon the cones. We considered the extent to which this undesired contrast could account for the BOLD fMRI signals we observed in response to a melanopsin-directed spectral pulse. For each subject, multiple measurements of the 400% melanopsin-directed stimulus spectrum were made before and after each data collection session. This set of measurements was averaged for each subject to produce a single spectrum, which was then submitted to a calculation (<https://github.com/spitschan/SilentSubstitutionToolbox>) that estimated the degree of contrast upon each of the post-receptor cone mechanisms (L–M, S, LMS). The four large, blue circles in each plot indicate the calculated contrast caused by device imprecision for the stimuli seen by each of the observers.

We created a stimulus modulation ("1x splatter"; Figure S1a) that had cone contrast equal to the max, across-subject contrast attributable to device imprecision. A set of "splatter" stimuli with log-spaced intensity ($\frac{1}{4}x$, $\frac{1}{2}x$, $1x$, $2x$) were derived from this initial modulation and studied during a control BOLD fMRI experiment. The spectrum of the 2x modulation was measured for each experimental session for each subject, and the cone contrast estimated in this modulation is indicated by the large, green circles (one circle for each observer; some plot symbols are overlapped).

We next considered how biological variability could cause these estimates of cone contrast to change. Our model of cone contrast incorporates assumptions regarding: lens transmittance; density of macular pigment; L, M, and S cone density; and variation in the peak spectral sensitivity (λ_{max}) of the L, M, and S cones. We simulated biological variation in these parameters by conducting 1,000 re-calculations of the cone contrast for each subject, using values for each parameter drawn from published distributions of individual differences.² The cone contrast returned by each simulation comprises a point in the cloud of blue values in each plot; an ellipse (solid line) indicates the iso-probability contour that encloses 95% of the 2D projection of the bootstrapped values upon the post-receptor axes, computed assuming that the underlying distribution was a bivariate Gaussian. The marginal distribution of this set of simulated contrast values is shown on each cardinal axis. The same calculation was conducted for the 2x splatter spectra, yielding the cloud of green points. [continued next page]

Figure S5: Inadvertent cone contrast in the fMRI stimuli – continued. We next related these values to our BOLD fMRI measurements. We have for each subject a contrast response function (CRF) for melanosin and for multiples of inadvertent cone contrast (splatter) due to device imprecision (Figure 3). For each subject, we asked how much larger the splatter contrast would have to have been to produce responses that match the melanosin CRF; this amounts to asking how many log-units the splatter CRF must be shifted to the left to best match the melanosin CRF (inset, bottom left). Across subjects, the mean shift multiplier was 4.1 (individual values were ASB 3.2, ASO 2.8, GKA 7.7, MXS 4.1). Extending the line that connects the origin of the cone-contrast space and the 2x splatter modulation, we identified the position that would correspond to a 4.1x splatter modulation (green hexagon). We considered the position of this point (and its mirror symmetric reflections) in the opponent modulation space with respect to the marginal distributions of simulated inadvertent contrast due to biological variability and device imprecision. The key observation is that the inadvertent cone contrast necessary to produce the observed BOLD fMRI responses to the 400% melanosin stimulus are unlikely to have occurred. The proportion of simulated contrast values (in both tails) that exceed the 4.1x level is 0.2% on the LMS dimension; 0% on the S dimension; and 5.3% on the L–M dimension. To account for our data, one or more of these values would have to have been exceeded for all four subjects. The odds of this occurring for a single subject is: $P(\text{LMS or L–M exceeded}) = 1 - ((1 - 0.053) \times (1 - 0.002)) = 0.0549$ and the odds of this occurring for all four subjects is $p = 9.1 \times 10^{-6}$. **(b)** The corresponding calculation of cone contrast due to device imprecision and biological variability for the melanosin stimulus used in the 400% contrast only experiment.

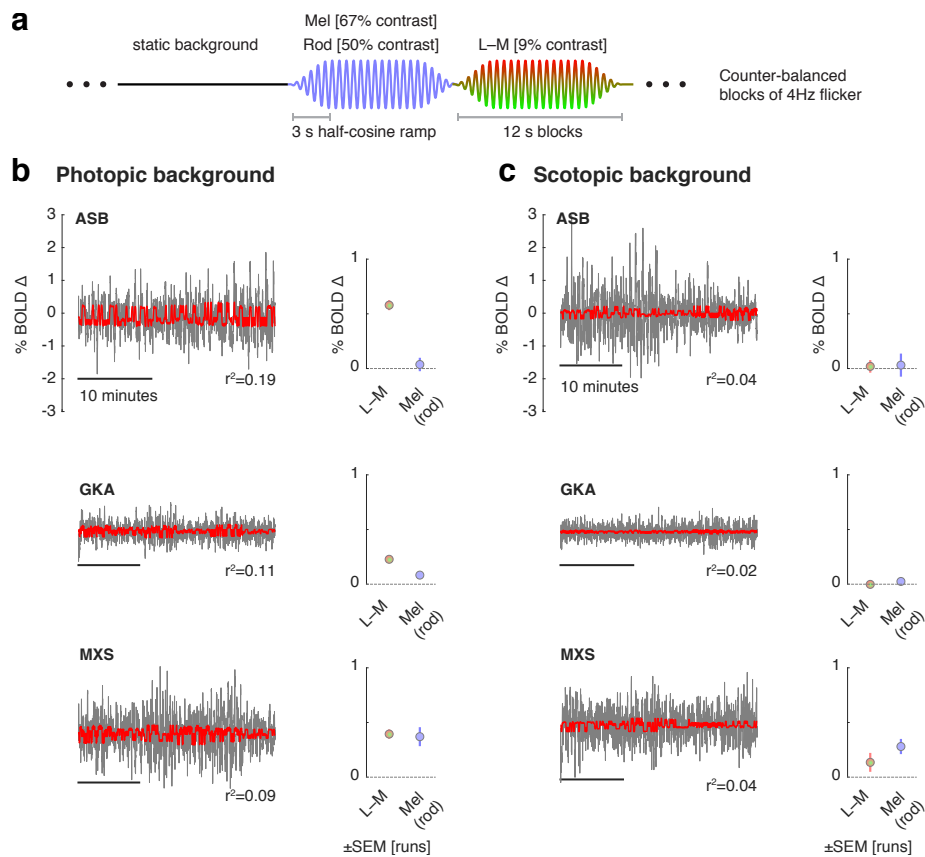


Figure S6: An unsuccessful control experiment (related to Figure 3). The rod and melanopsin spectral sensitivity functions overlap extensively. The background used for our melanopsin directed stimuli was $3.5 \log_{10}$ scotopic Trolands (scot Td), nominally at or above the rod saturation threshold, found to be $3.0 \log_{10}$ scot Td (Figure 2 of Adelson 1982)³ or $3.3\text{-}3.7 \log_{10}$ scot Td (Aguilar & Styles 1954).⁴ Therefore, we may expect in our experiments that there is no, or minimal, time-varying signal contributed by the rods. Nonetheless, we considered control experiments that could address the possibility of rod intrusion. While it is possible in principle to create a melanopsin directed stimulus that silences both the rods and cones, in practice we find that our device is limited to a maximum 60% unipolar (Weber) contrast pulse directed at melanopsin while silencing both rods and cones. Given our finding that at least 100% unipolar melanopsin contrast is needed to produce a reliable cortical response, we regarded this stimulus as ineffective. Instead, we examined whether the response to our melanopsin directed stimulus varied as a function of temporal frequency, with the logic that melanopsin responses would be attenuated to a stimulus modulated at 4 Hz, while rod responses would persist. Ultimately we found this experiment to be uninformative. The BOLD responses evoked by the stimuli were small and / or poorly modeled, with low r^2 values, particularly in the scotopic condition. Moreover, inconsistent responses were obtained across subjects. Despite our inability to draw clear conclusions from these measurements, we present the data here for completeness. **(a)** The experimental design was adapted from a prior study.⁵ Around a common background, we presented a 4 Hz modulation that targeted either L–M with a 9% bipolar (Michelson) contrast (while silencing the rods) or melanopsin with 67% bipolar contrast on melanopsin and 50% bipolar contrast on rods. The modulations were presented in 12 s blocks, with a 3 s half-cosine window at onset and offset, in a counter-balanced order. **(b)** Photopic conditions. *Left* The BOLD fMRI time-series data from the area V1 region for each subject (black), following pre-processing to remove nuisance effects. The data were modeled (red) with a step-function for each stimulus condition, convolved by subject-specific hemodynamic response function. *Right* The amplitude of evoked responses for each subject for the 4 Hz L–M and melanopsin modulation blocks as compared to the static background. **(c)** The corresponding data obtained during scanning under scotopic conditions. Subjects dark-adapted for at least 20 minutes prior to scanning. A 6 log unit neutral density filter was placed in the light path, reducing the stimulus background to approx. 0.0001 cd/m^2 .

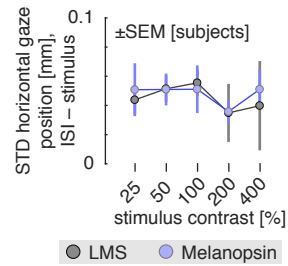


Figure S7: Variation in horizontal gaze position with stimulation (related to Figure 4). Subjects were asked to maintain fixation upon the center of a 5° opaque circle. Infrared video of the left eye was recorded during functional MRI scanning in some experiments. We measured the horizontal position of the eye during the scanning session to examine if stimulus presentation led to systematic changes in fixation stability. While vertical eye position was recorded, these data were not considered given that the eye has less fixational variation in the vertical plane, and the generally noisier quality of the vertical position data. The standard deviation of eye position was measured during the three seconds of stimulus presentation and during the ensuing interstimulus interval (ISI). The mean difference (averaged across subjects) between the ISI and stimulated periods was obtained for the LMS (gray) and melanopsin (blue) stimuli at each contrast level. A clear effect of stimulation was to reduce horizontal eye movement as compared to the ISI period (all data points different from zero). This effect did not systematically vary by stimulus type (LMS or melanopsin) or by contrast. Therefore, differences in BOLD fMRI responses between contrast levels or stimulus type are not explained by differences in evoked eye movements. It remains possible, however, that measured cortical responses to stimulation contain some constant component of change in eye movements. This effect may contribute to prior results.⁶

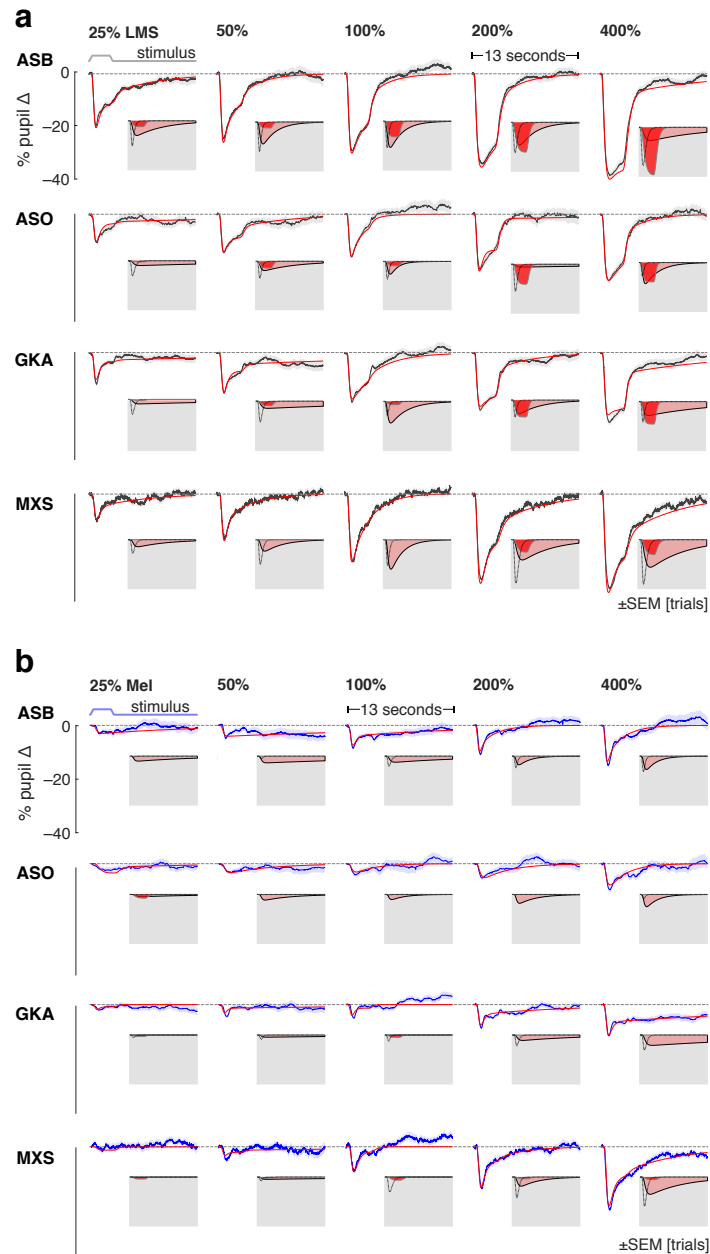


Figure S8: Individual subject pupil responses (related to Figure 4). The consensual pupil response of the left eye was measured during stimulation of the pharmacologically dilated right eye. **(a)** The mean (across trials) pupil response evoked by LMS stimulation of varying contrast levels (black), with SEM across trials (shaded). Each row contains the data from a different participant. The evoked response was fit with a three component, six-parameter model (red). The three components that model each response are shown inset on a gray field. **(b)** The corresponding mean pupil responses evoked by melanopsin stimulation of varying contrast levels.

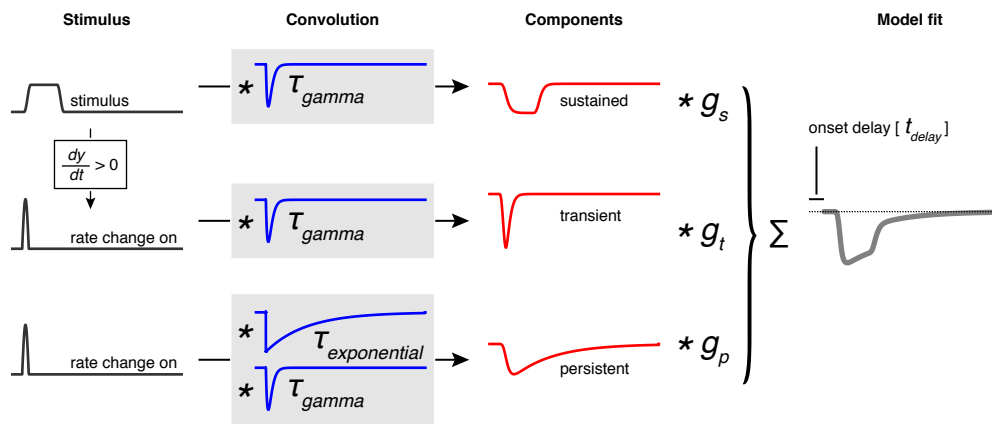


Figure S9: Pupil temporal model (related to Figure 4). The across-trial, within-subject average evoked pupil response to each stimulus type (LMS and melanopsin) and contrast level was fit with a six-parameter, three-component model using a non-linear temporal fitting engine (<https://github.com/gkaguirrelab/temporalFittingEngine>). The model was designed to capture the three, visually apparent and temporally separated components of the evoked pupil response. The elements of the model are not intended to directly correspond to any particular biological mechanism. The input to the model was the stimulus profile (black). An additional input vector, representing the rate of stimulus change at onset, was created by differentiating the stimulus profile and retaining the positive elements. These three vectors were then subjected to convolution operations composed of a gamma and exponential decay function (blue), each under the control of a single time-constant parameter (τ_{gamma} and $\tau_{\text{exponential}}$). The resulting three components (red) were normalized to have unit area, and then subjected to multiplicative scaling by a gain parameter applied to each component ($g_{\text{transient}}$, $g_{\text{sustained}}$, and $g_{\text{persistent}}$). The scaled components were summed to produce the modeled response (gray), which was temporally shifted (t_{delay}). We observed that some evoked responses for some subjects had a late dilation phase in which the pupil became larger than its baseline size. We did not attempt to capture this inconsistent behavior in our model.

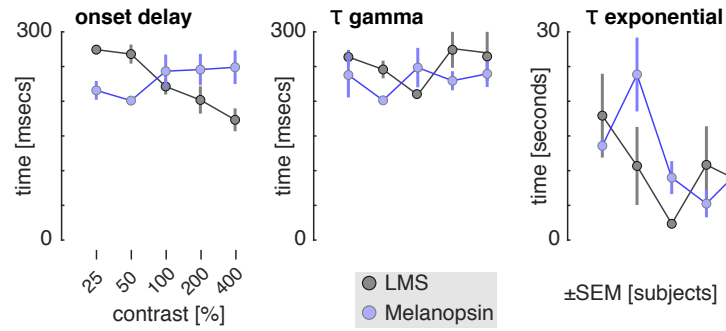


Figure S10: Temporal pupil model parameters by contrast (related to Figure 4). Pupil responses were fit with a six-parameter model, of which three parameters controlled the temporal behavior of the model. Each plot presents the mean (across subjects) of a temporal parameter, as a function of contrast for LMS (gray) and melanopsin (blue) stimulation.

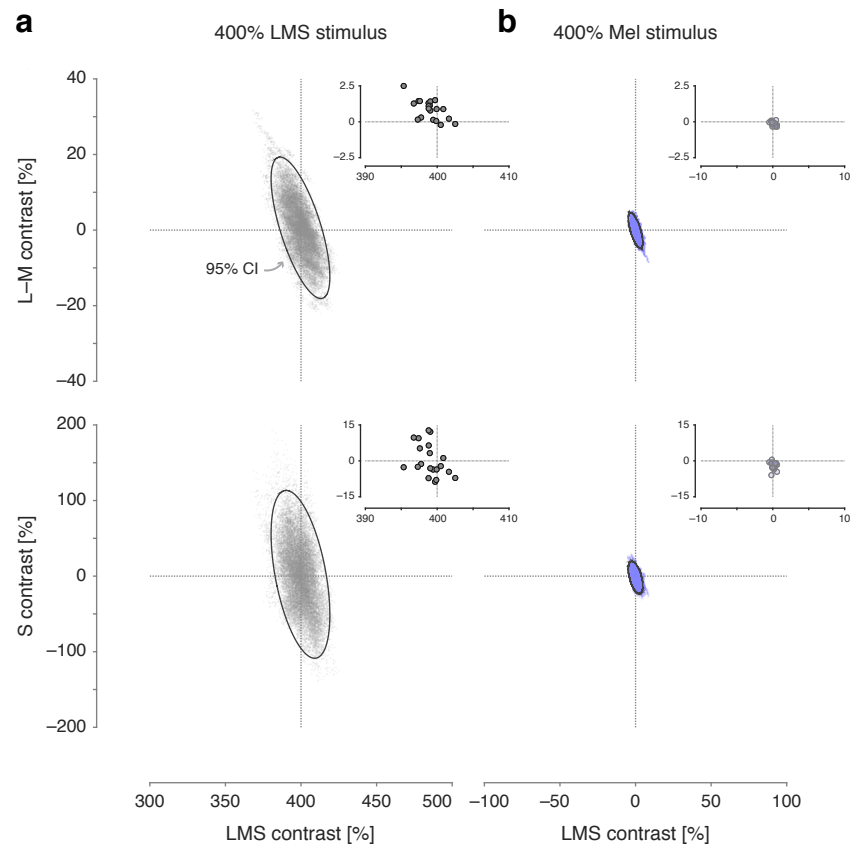


Figure S11: Inadvertent cone contrast in the perceptual stimuli (related to Figure 5). *Inset* in each plot is the calculated post-receptoral cone contrast of the melanopsin and luminance 400% spectral pulses used in the perceptual experiment. Each point corresponds to the difference between the background and stimulus spectra measured for each subject at the time of their testing session. Following the same procedure as described in Figure S5, we then simulated the post-receptoral cone contrast that might be produced by our stimuli in the face of biological variability in our subjects. **(a)** Post-receptoral contrast estimated from simulations for the 400% LMS (luminance) stimulus. **(b)** Post-receptoral contrast estimated from simulations for the 400% melanopsin stimulus.

<i>quality</i>	<i>melanopsin</i>	<i>LMS</i>	<i>Light flux</i>
	median \pm	inter-quartile	range
cool to warm	4.25 \pm 4.00	4.50 \pm 2.00	4.5 \pm 1.25
dull to glowing	4.50 \pm 3.75	5.00 \pm 1.25	5.5 \pm 2.50
colorless to colored	5.75 \pm 1.25	3.25 \pm 2.25	2.0 \pm 1.50
focused to blurred	5.00 \pm 1.75	3.50 \pm 3.00	3.5 \pm 2.25
slow to rapid	4.00 \pm 2.50	4.75 \pm 2.00	4.5 \pm 1.75
pleasant to unpleasant	4.75 \pm 2.75	3.00 \pm 2.00	3.0 \pm 1.50
dim to bright	2.50 \pm 3.25	5.25 \pm 1.50	6.0 \pm 1.25
smooth to jagged	3.50 \pm 2.75	2.25 \pm 1.75	2.0 \pm 1.50
constant to fading	5.00 \pm 2.50	2.00 \pm 1.75	2.0 \pm 1.50

Table S1: Across-subject ratings of nine perceptual qualities for 400% contrast pulses of the three stimulus types.

melanopsin

Lot of difference between surrounding of dot (fixation dot) and periphery. Space around dot, red-orange to lighter orange. Cloudy thing around dot, ignoring it for periphery. Difference between center and periphery large and distracting. Looks like a lava lamp. Lava changes shape between pulses. (MELA.0026)
Appeared distinctly red - maxwell spot appeared very red. Faded to the black that is the noise when your eyes are closed about a dots (fixation dot) width away from the center. (MELA.0037)
Definitely looks reddish around the ring of the fixation dot, further into the periphery not so much. Hard to describe. (MELA.0038)
Pulses were disorienting. Kind of like if you got hit in the head really sharply. Experience kind of like flashing lights and fade out. Pulses were more green than other two types of runs. Other two runs were orange-ish. (MELA.0043)
Huge transition from background to pulse. Went from a yellow to grey color, but the pulse still contained color aspects of the background. (MELA.0049)
Pulse was so gradual that couldnt tell its changing color. Felt a bit like the pulse was straining their eye compared to the background. Pulses looked pink-red and magenta. (MELA.0073)
Like a psychedelic; unnatural; stimulus that they rarely experience. The psychedelic and foreign, less familiar. More shimmering, corresponds to psychadelicness. (MELA.0074)
Looked more different than the other two (light Flux and LMS). Background was green, pulse was closer to red. Harder to focus on too. Green background was red towards the middle. Less harsh than first time seen. (MELA.0075)
Did see maxwell spot extend beyond the edge of the black fixation dot. Pulse was very strange color- did not know what color it was. Trouble describing color. (MELA.0080)
Pulses looked similar to each other, appeared green. Pulses has same brightness and same onset time. (MELA.0081)
Like looking at the sun. Coloration looks like the sun, NOT uncomfortable. Felt like a faded version of sun. (MELA.0082)
Like blinding in a sense. Switches between white and black, not uncomfortable. Not really any color. (MELA.0088)
Very similar in color to first run, but the onset is different against background. Background seems different: looks like it has less color, says they know it is orange but it looks more bland in the first run. (MELA.0090)
Fairly unpleasant. Seemed really harsh, like staring at something really bright. Automatically wanted to blink. uncomfortable but not painful. Discomfort because of brightness. Really aversive, super harsh. Made them want to blink. Very bright. (MELA.0094)

luminance

See a very thin but very bright ring around black circle- very red. Red ring still there - becomes more defined longer they stare at background. (MELA.0026)
lighter version of peach stimulus. Seemed more faded along edges. Seemed similar to pulse before last (Light Flux). (MELA.0037)
Uniform, sort of whitish pulse/intensity change (MELA.0038)
Started off as background, seemed like Light flux background, but by the third rating (colorless to colored) background seemed yellow with pink pulse. Seemed like a less bright version of Light Flux. The background remained yellow with specks of pink. Adaptation was yellowish in hue. (MELA.0049)
If compared to first pulse, less brightness, color didnt change as much and more dull. Seemed clearer but less bright. (MELA.0050)
Seems like the pulse is a cooler, lighter version of the background. Comfortable to look at. Was cooler than background and more white-toned than background. White toned meant the pulse was faded to a lighter version of the background, the brightness was different. (MELA.0073)
Pretty comforting, benign, friendly, familiar. Strong but comfortable, very luminous. (MELA.0074)
Looked similar to light flux in terms of color but dimmer. Like last run (Light flux) but not as bright, seemed less harsh. (MELA.0075)
Focused to blurry is difficult: didnt notice any particular focusedness or blurriness. (MELA.0077)
Perceived it as the same as Light Flux. Seemed similar to other runs except Mel. (MELA.0080)
Pulses were all the same color and brightness, did not state what color pulses were. Pulses appeared identical. (MELA.0081)
Like the first run (Light flux) but better. Felt like it was hazy or foggy. Color was the same, just foggy. Eye piece was not foggy. (MELA.0082)
Kind of brownish gray pulse. Kind of colorless, similar to last run (LF) (MELA.0088)
Feeling desensitized to brightness, these pulses didnt seem as bright as first time though the color was the same. (MELA.0090)
Roughly similar to first pulse - less colorful than first one in terms of absolute color. Most other aspects seemed pretty similar. Looks neutral like other rounds. Very bland and pastel-ish. (MELA.0094)

light flux

Pulse looked peachish in color. More pinkish than first run LF and run 1 LMS. (MELA.0037) Looked like a uniform whitish intensity increase, nothing really stood out. (MELA.0038) Color was warm, because it was close to red. The pulse of light was uncomfortable. Thought of neon light. Part of the pulse was blurry at first, but they could then perceive the constancy of the pulse. Similar to first run. It seem a little more clear than first run. (MELA.0049) Pulse felt more concentrated (meaning opaque) towards center, and almost blurry. Somewhat more blurry than previous pulses. (MELA.0050) Rated smooth to jagged in regards to the onset/transition of the pulse from the background. The pulse is more comfortable to look at than the background. Was bright but not uncomfortable. Pulse was a lighter version of the background. (MELA.0073) Pretty friendly. Seemed bright in intensity and character. Very illuminant. (MELA.0074) Everything was kind of blurry, so it was difficult to make ratings. Pulses seemed the same the whole way through. More similar to LMS and Light Flux than to melanopsin. (MELA.0080) Seemed like a light pink light that came on and off. Wintery: like the kind of light expected during a pretty winters day. Kind of like light off of snow. Feels like all of the pulses are constant. (MELA.0082) Pink and somewhat bright pulses. Kind of a dull orange, kind of colorless. (MELA.0088) Pulses appeared neutral- seemed like a wall in a building - like a hospital or an office building. After the pulse goes away subject had trouble seeing until they blinked- might be that they were unable to focus, not totally sure. Fairly pretty, pleasant, neutral-ish. Most of the properties, hue and brightness and aversiveness were very neutral. Like vanilla. (MELA.0094) Pulse looked white, so rating colorless to colored was weird. Smooth to jagged was hard to rate. Pulse looked white again, colorless. For colorless to colored the rating reflected the change from the background. (MELA.0096)

Table S2: Free-form descriptions of the pulsed stimuli

Subjects in the perception experiment were invited to describe their impressions of the stimuli during a debriefing session and these were recorded by the examiner. Subject ID codes given in parentheses. The subject was not told the spectral identity of the stimuli, and in their descriptions referred to the stimuli by their experimental order; these references to run order are replaced here by the spectral identity of the stimulus for clarity. Some subjects provided descriptions of changes in the appearance of the stimulus at the edge of the masked macular region; they were asked to ignore this aspect of the stimulus in their ratings.

URL	Experiment name and protocol deviations
https://osf.io/yzwm6	fMRI Expt 1, 400% Mel pulses <ul style="list-style-type: none">- Pulse-oximetry regressors were not used due to an error in the date field of the timestamps of the physio files. We discovered this error during a code audit after completing the analyses presented here. While it would be possible correct for this error in data analysis, we elected to not re-process our data to include the physiologic regressors, as these explain minimal variance within occipital cortex.- A Fourier basis set instead of an FIR basis set was used to model the fMRI data, given the asynchronous timing of events relative to TRs- The V1 region of interest was set to 5–25° (as opposed to 5–30°) as we wished to have additional stringency in avoiding signals from beyond the boundary of the stimulated field (which could contain rod intrusion)- Preliminary analyses of the LGN region of interest showed poor quality signals, so this was not pursued further- We have not pursued analyses of the extra-striate regions of interest
https://osf.io/vqady	fMRI Expt 2, 400% LMS pulses. Deviations as described for Experiment 1, and <ul style="list-style-type: none">- The double-gamma model was found to produce poor fits to the evoked responses. This approach was discarded in favor of estimation of the shape of the HRF in individual subjects, and the use of the neural-step function model.- A proposed analysis would have examined differences between the LMS and Mel stimuli in evoking responses within the cortical and subcortical somatosensory system. These analyses have not yet been pursued.
https://osf.io/ayvb5	fMRI Expt 3, Splatter CRF. Deviations as described for Experiment 1.
https://osf.io/w86pu	fMRI Expt 4, Mel CRF. Deviations as described for Experiment 1.
https://osf.io/w95da	fMRI Expt 5, LMS CRF. Deviations as described for Experiment 1.
https://osf.io/pv3a4	fMRI Expt 6, Rod control. While pulse oximetry data were collected, these were not used so that the analyses of these data matched the analyses performed for the other experiments.
https://osf.io/u8ggn	Perceptual rating of Mel and LMS pulses <ul style="list-style-type: none">- A set of 5 pre- and 5 post-experiment, validation measurements of the stimulus spectra were made and averaged. A small subset of these measurements (3 out of 750) featured clearly abnormal spectra due (we suspect) to a transient failure of device control. We excluded these spectra from the average that was generated across the validations.

Table S3: Pre-registrations and protocol deviations

Links are to pre-registration pages on the Open Science Framework site. Some pre-registrations include addenda.

References

1. CIE. Commission Internationale de l'Eclairage Proceedings. Cambridge, UK: Cambridge University Press; 1932.
2. Asano Y, Fairchild MD, Blondé L. Individual Colorimetric Observer Model. PloS one. 2016;11(2):e0145671.
3. Adelson EH. Saturation and adaptation in the rod system. Vision research. 1982;22(10):1299–1312.
4. Aguilar M, Stiles W. Saturation of the rod mechanism of the retina at high levels of stimulation. Journal of Modern Optics. 1954;1(1):59–65.
5. Spitschan M, Datta R, Stern AM, Brainard DH, Aguirre GK. Human visual cortex responses to rapid cone and melanopsin-directed flicker. Journal of Neuroscience. 2016;36(5):1471–1482.
6. Hung SM, Milea D, Rukmini AV, Najjar RP, Tan JH, Viénot F, et al. Cerebral neural correlates of differential melanopic photic stimulation in humans. NeuroImage. 2017;146:763–769.